HEAT AND MASS TRANSFER

IN COLD REGIONS SOILS

by

Douglas L. Kane
Assistant Professor of Water Resources
University of Alaska

James N. Luthin
Professor
University of California, Davis

and

George S. Taylor
Professor
Ohio State University, Columbus

Institute of Water Resources
University of Alaska
Fairbanks, Alaska

Report No. IWR No. 65 June 1975

ACKNOWLEDGEMENTS

The work upon which this report is based was made possible by a cooperative aid agreement between the U.S. Forest Service, Institute of Northern Forestry, Fairbanks, Alaska, and the Institute of Water Resources, University of Alaska. Contributions to this study were also made by the University of California at Davis and Ohio State University. The collection of winter data on pore pressures was made possible by a separate grant by the Office of Water Research and Technology (project A-053 ALAS).

The authors appreciate the help of Wolfgang Hebel, Richard Seifert, and Roberta Jones in collecting and compiling the data; Mayo Murray for editing the manuscript; and Judith Henshaw for drafting the figures.

TABLE OF CONTENTS

LIST OF FIGURES

INTRODUCTION

Many parts of interior Alaska have a fire-dominated environment. Annually about one million acres of forest land are burned throughout the state. The more intense burns occur in the black spruce (*Picea mariana*) forests which are characterized by a thick organic layer and a shallow mineral soil underlain by permafrost. The result of a fire in a black spruce setting is the immediate destruction of the tree, lichen and moss, and surface organic layers. The degree of disturbance depends upon the intensity of the burn which is related to wind, temperature, humidity, soil moisture, type and quantity of fuels, and topography. This change in the surface boundary caused by fire is reflected in several heat and mass transfer processes of interest.

The trend over the past three decades in Alaska has been an increase in the number of fires, but a decrease in the total acreage burned (Barney, 1971).

Time	No. of Fires	Total Acreage Burned	Average Acreage/Fire
1940-1949	1138	12.4×10^6	10,906
1950-1959	2583	10.7×10^6	4,137
1960-1969	2380	6.4×10^6	2,674

Lightning accounts for only 30% of the individual fires; however, these fires account for almost 80% of the area burned. More efficient methods of fire prevention and control are reflected by the substantial reduction in total acreage burned in the last decade.

Wright and Heinselman (1973), in discussing the ecological role of fire, listed six generalized effects: influence on the physical and chemical environment; regulator of dry matter accumulation; controller of plant species and communities; determinant of wildlife habitat patterns and populations; controller of forest insects, parasites, and fungi; controller of major ecosystem processes and characteristics. Many of these categories overlap and therefore are not completely separable. Discussion in this paper will deal only partially with the influence on the physical environment and more specifically with the thermal and moisture regimes of the near-surface soils.

The objectives of this study were to examine the soil moisture and temperature conditions in a burned and an unburned area in a black spruce forest. Presented in this paper are the results of one year of data collection; the same data for an area burned in 1971 are also included. Field data results are complemented by both a conceptual presentation of changes induced by fire and a mathematical model describing the drainage characteristics of the near-surface organic layer.

The preliminary results of this study indicate that major changes do occur in the physical system resulting from fire manipulation, both in the thermal and moisture regimes. An understanding of heat and mass transfer dynamics is vital to any meaningful understanding of biological and chemical system dynamics, as well as the hydrologic system. Changes in the hydrologic system are more apparent at the air/ground interface, although almost all facets are influenced.

CONCEPTUAL MODEL

Fire in subarctic forests produces a series of changes in soil conditions and in the vegetative cover. The time sequence of events following a fire is important if fire is to be used as a forest management tool. In order to improve our analysis of this sequence, the following conceptual model is presented (Figure 1). The purpose of the model is to focus attention on sequential events of importance in order that fires can be planned. The model is an outgrowth of an earlier model proposed by Luthin and Guymon (1974).

The most obvious effect of fire is on the canopy of trees. However, a more significant effect may be the partial or complete destruction of the organic layer found at the soil surface. The thickness of this organic layer

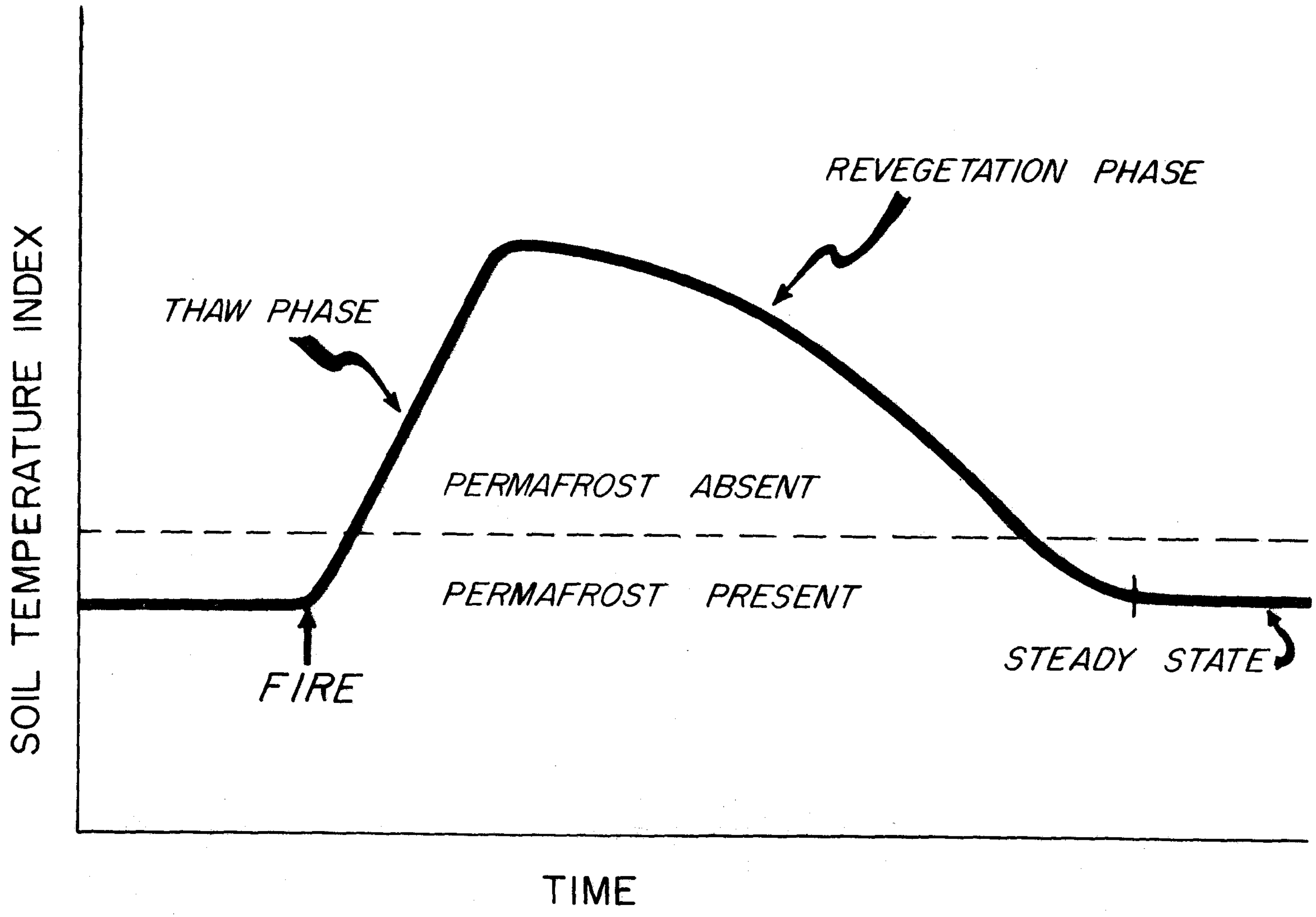

FIGURE 1: Conceptual Model Illustrating the Changes in the Thermal State at a Given Depth Preceding a Fire.

is variable but in many places it is 20 to 25 cm thick. Both the canopy and the organic layer serve to insulate the mineral soil from incoming radiation during the summer.

The presence of the canopy and the organic layer reduces the average annual mineral soil temperature. Destruction of these by fire causes an increase in the average annual soil temperature. The degree to which the canopy and organic layer are removed during the fire event is a function of the intensity of the fire.

After the fire event, the average annual soil temperature rises due to the destruction of the canopy and partial destruction of the organic layer. An additional factor affecting the thermal regime will be the site aspect. Incoming radiation is, in part, a function of the aspect of the site.

After the fire event, a new vegetative sequence is established. The improved soil temperature conditions lower the permafrost table and improve the soil moisture situation. The result is a warmer soil with greater depth to the permafrost table.

The situation is conducive to the reestablishment of a vigorous vegetative cover. As the canopy develops and the organic layer begins to regenerate, a situation develops which is conducive to a reduction of the average annual soil temperature. The burned area starts to revert to its original pre-fire condition - shallow permafrost and waterlogged soil - which severely restricts vegetative growth.

In a forest management program, it is important to be able to quantify the time sequence of the events described above. As an initial effort in this direction, the conceptual model (Figure 1) was prepared. The exact functional relationship is not known. Also the magnitude of the changes is unknown. This is only a pictorial representation of the sequence of events related to a fire. Efforts should be directed toward a quantification of the events. Hopefully, the graph will help to direct research efforts into fruitful measurements.

The sequence of events preceding and following a fire can be characterized as follows:

Phase I - Steady state phase.

This is the condition that establishes itself in a stand of black spruce that has been protected from fire for long periods of time. A thick layer of organic matter is present on the soil surface. The soil thermal "index" is at its lowest point. The exact value of this index will depend to some extent on the aspect of the site. As used here, the exact nature of the soil thermal index is not defined and current research is directed toward the establishment of an index which will characterize the soil thermal regime. Permafrost may or may not be present at this time although there is an excellent likelihood of its presence.

Phase II - Post-fire phase of increasing soil temperature.

The fire destroys the canopy and partially destroys the organic layer. The degree to which the organic layer is destroyed is largely dependent upon the fire intensity. Practical information is needed relating fire intensity to organic layer destruction since the organic layer plays a very significant role in controlling the soil thermal regime. In this phase, the soil temperatures rise and revegetation starts. We need quantitative information on the soil thermal regime during this period as a function of organic layer destruction.

Phase III - Revegetation phase.

Revegetation starts soon after the fire event. However, it is some time before the soil thermal regime starts downward again. Research is needed to describe this period in quantitative terms. It will be influenced by the rate of revegetation and by the rate at which the organic layer reestablishes itself. As this happens, the soil thermal regime declines until eventually we are back at steady state with permafrost, waterlogged soils, and reduced plant growth.

SETTING AND INSTRUMENTATION

Washington Creek watershed (Figure 2) is typical of interior Alaska watersheds. This entire area is generally considered to be in a zone of discontinuous permafrost bordered on the north by the Brooks Range and extending almost to the southern coast. In some areas, permafrost may be absent; in others it may exist 50-100 cm below the ground surface. In addition to the importance of permafrost, an organic layer over the mineral soil is very important. This layer appears to act as a buffer to both heat and moisture flow with the maximum thickness of this layer exceeding 30 cm. The physical picture presented here is one of a two- or three-layered system with varying properties: organic layer, mineral soil, and possible permafrost.

At the study sites, the organic layer in the unburned areas is 20-25 cm thick and, in the burned areas, the residual thickness is about 5 cm. The mineral soil is composed of a variety of silt loams deposited over a highly weathered schist (Furbush and Schoephorster, 1974). Black spruce is the principal tree type in this area, although mixed forests (birch, aspen, white spruce) do exist in well-drained areas.

Six plots were instrumented. Two plots (N-1, N-2) were situated on an east-west ridge in a 1971 burn site; two plots (S-1, S-2) were located on the same ridge in the unburned forest; and two plots (BS-1, BS-2) were placed in a undisturbed black spruce permafrost setting at a lower elevation with poor drainage. The main field data collected were snowpack-organic layer-mineral soil temperatures throughout one year and soil pore pressures, primarily in the mineral soil, for the period August through December. Basic instrument positioning is illustrated in Figure 3. Other measurements included soil moisture content, air temperature, snowpack depth and density, summer precipitation, seasonal frost depth, and delineation of permafrost boundaries.

The tensiometers used to measure pore pressure consisted of a porous cup attached to either a mercury manometer or a vacuum gauge. The main reason for

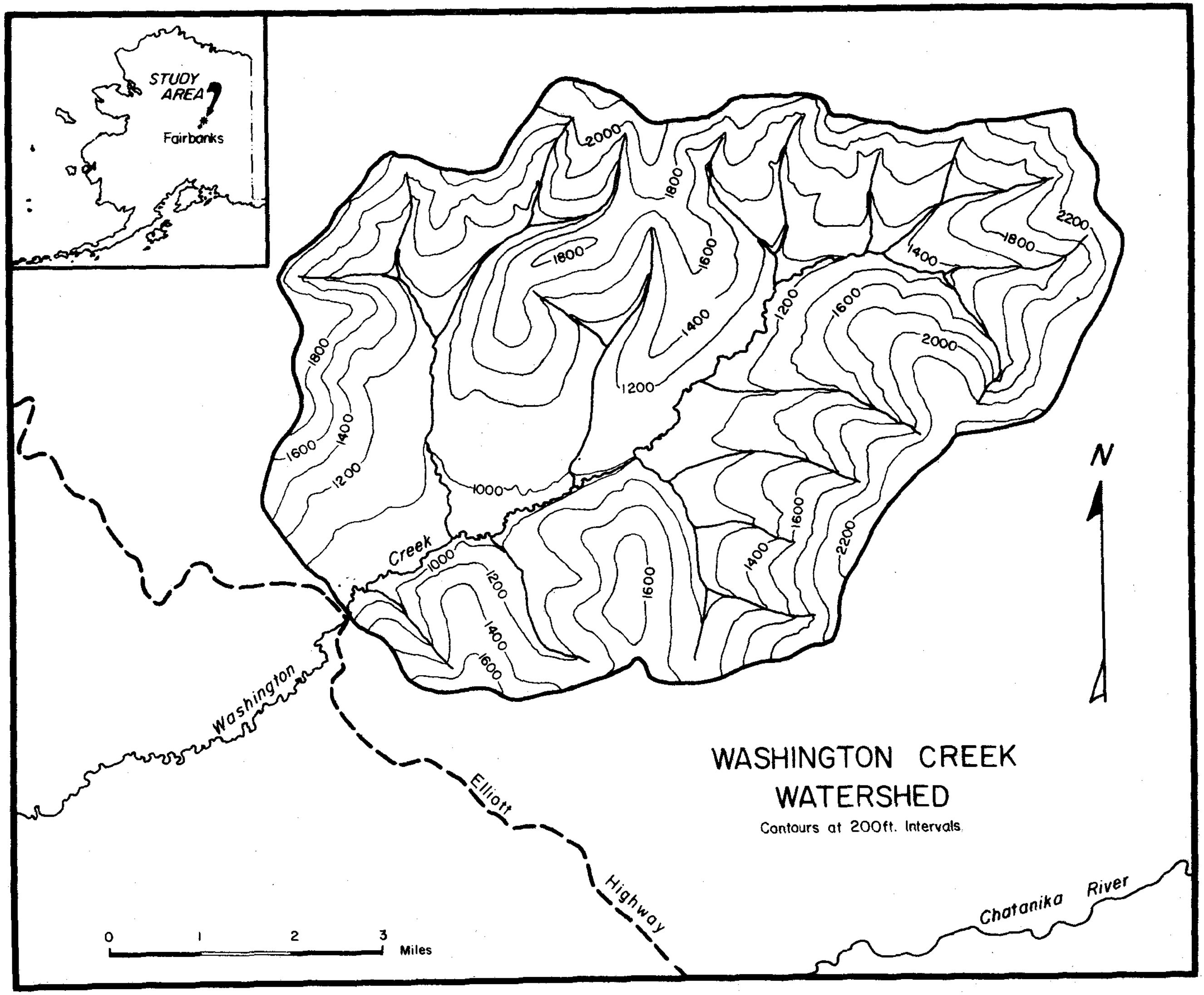

FIGURE 2: Location and Topographic Map of Washington Creek Watershed.

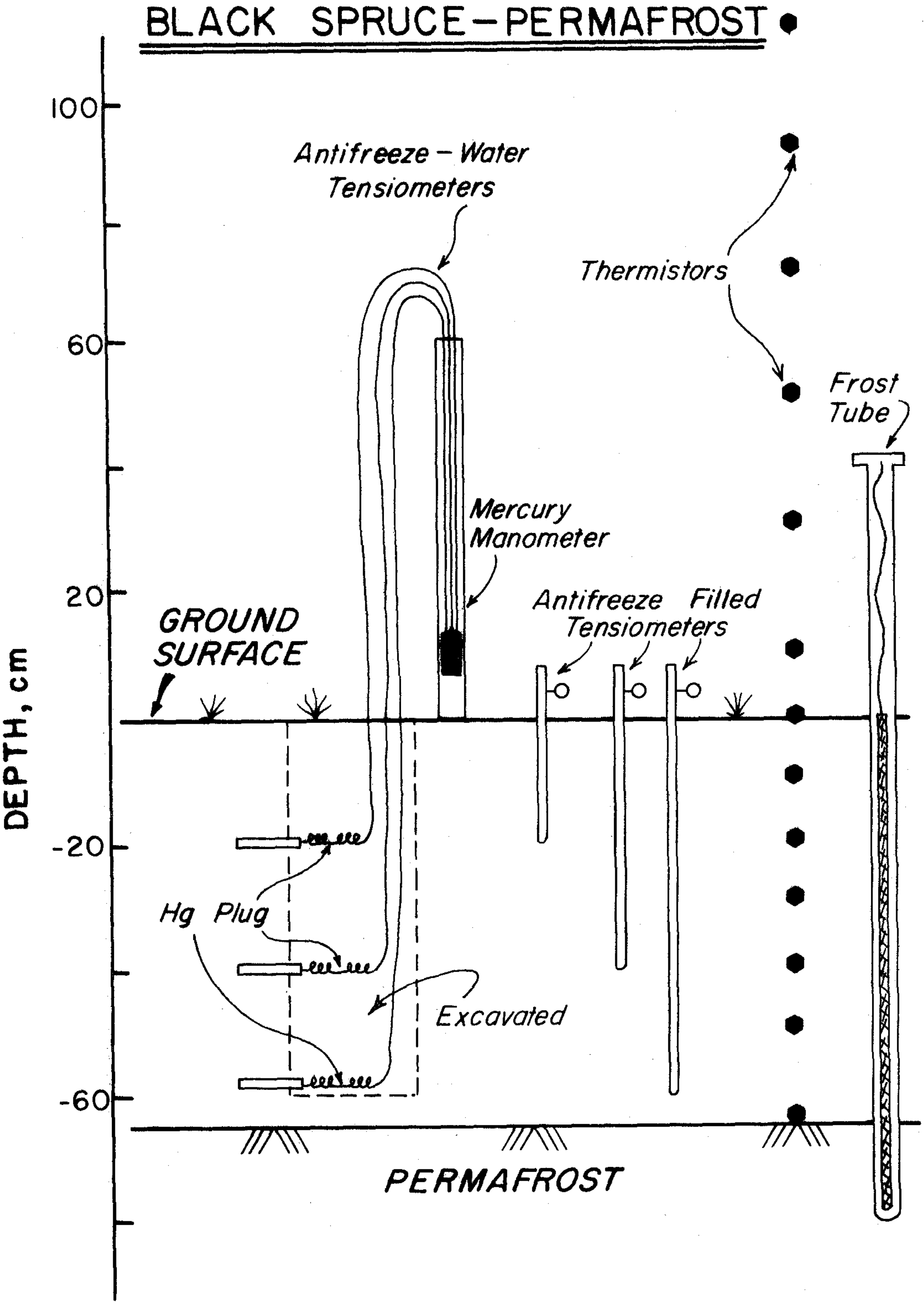

FIGURE 3: A Typical Instrumented Site.

collecting soil tension data is to predict soil water movement. The vertical flux of water can be determined from the following equation:

$$V_z = K(z, \theta) \frac{\partial \phi}{\partial z} \qquad (1)$$

where

$K(z,\theta)$ = hydraulic conductivity of the soil at depth z and soil moisture content θ

ϕ = hydraulic head = $-(\psi+y)$

ψ = matrix potential

Assuming the osmotic and electrical potentials are minimal, the matrix potential is the value indicated by the tensiometers. Once the correction is made with regard to the position of the tensiometer cup in the soil column, the hydraulic gradient $(\frac{\partial \phi}{\partial z})$ can be defined. No attempt was made to determine the hydraulic conductivity in the laboratory for these soils. Numerous methods for estimating hydraulic conductivity of unfrozen soils are available. Additional work is needed to determine the hydraulic conductivity of frozen soils and their relationship with moisture content and temperature. In natural settings, the unsaturated hydraulic conductivity varies considerably for two reasons: the vertical variation of the moisture content and the non-isothermal conditions that exist in frozen soils. It would seem that there would be a substantial reduction of the hydraulic conductivity in frozen soils where ice crystals occupy spaces in the soil matrix. However, this same freezing process is responsible for very high negative hydraulic gradients, therefore the reduction in the quantity of flow may not be great.

In an attempt to measure pore pressures during the winter season, two techniques were tried. One was simply replacing the water in the tensiometers with a solution of ethylene glycol and water. Since the interaction of the antifreeze solution and the porous media is not known, the results of this method are questionable.

The second scheme consisted of filling a small tensiometer with water. The tube running to the mercury manometer was filled with an antifreeze solution. A mercury plug separated the two fluids to prevent mixing. A trench had to be excavated to install these tensiometers.

It has been reported that most of our tensiometers failed during December and January, a period of extremely low temperatures. It was assumed that the fluid in the tensiometers froze and subsequently cracked the tensiometers (allowing air to enter). When these instruments were removed in the spring, they were all found to operate perfectly. Apparently this large loss in fluid resulted from the extreme hydraulic gradients that developed. As the soil froze, large negative tensions developed in the frozen soil; once the air entry value of the tensiometer was exceeded, air entered the tensiometer, bringing it into equilibrium with the atmosphere. Since it is not in equilibrium with the soil, the fluid flowed from the tensiometer to reach equilibrium with the soil. When the soil tension was less than one atmosphere (negative), air again entered the tensiometer. Several such cycles soon removed all of the fluid in the instrument.

Fluorescein-filled frost tubes were used to determine the seasonal frost and permafrost boundaries. Thermistors with an accuracy of ±0.2°C were used for all but the air temperature measurements. Soil moisture contents for the mineral soil were determined by prescribed gravimetric methods. Soil samples high in organic matter were dried in a microwave oven in order to prevent oxidation of the organic material. This technique is discussed in a paper by Miller *et al.* (1974).

DISCUSSION OF DATA

The initial objective of this project was to collect some basic soil moisture and temperature data in a burned and an unburned forest setting. Washington Creek drainage has been proposed as an area for prescribed burns in the future; an adjacent area burned during July 1971. Site selection in Washington Creek drainage was based primarily on accessibility. Two sites were located on an east-west trending ridge on the north boundary of the basin. These two sites, accessible by a trail, were about 100 m apart. The third site was along the existing highway, 120 meters lower in elevation.

This study was envisioned as a long-term study with the preliminary data from the first year helping to formulate the main structure of the process. Later studies were to be more refined, addressing some of the more complex and unique elements of this soil environment. While this was meant to be a preburn study, it was felt that the instrumental plots in the burned areas would yield beneficial information. This data made it possible to compare temperature and moisture regimes, direct future data-collection for areas of prescribed burns, and develop a preliminary understanding of the impact of fire.

As previously mentioned, the bulk of the data collected consisted of temperatures (air-snow-soil), soil pore pressures, and soil moisture content. This data was collected at weekly intervals from July through December, 1974. At that time, pore pressure measurements were suspended and soil moisture samples were collected about once per month.

To date we have had very little chance to examine the hydraulic and thermal properties of the mineral and organic layers. Plamondon *et al.*, 1972, discussed the hydrologic properties of the forest floor for a setting north of Vancouver, British Columbia. The bulk density and thickness in these forest floors are comparable to the Alaska setting. The hydraulic conductivity was found to vary about four orders of magnitude over a range of matrix potentials between -.003 and -.08 bars and the layer stored a significant amount of rainfall. An understanding of these properties under frozen conditions is likewise needed. Williams and Burt (1974) describe a method for measuring hydraulic conductivity of frozen soils and discuss the variability of the hydraulic conductivity as a function of temperature for a frozen silt. Dingman (1971) looked at the water-holding and transmitting properties of the organic layer for a setting near Fairbanks.

Temperature Measurements

Temperature data collection was initiated during the middle of July, 1974 (Figures 4, 5, and 6). At that time, the ground had thawed to a depth of 55 cm

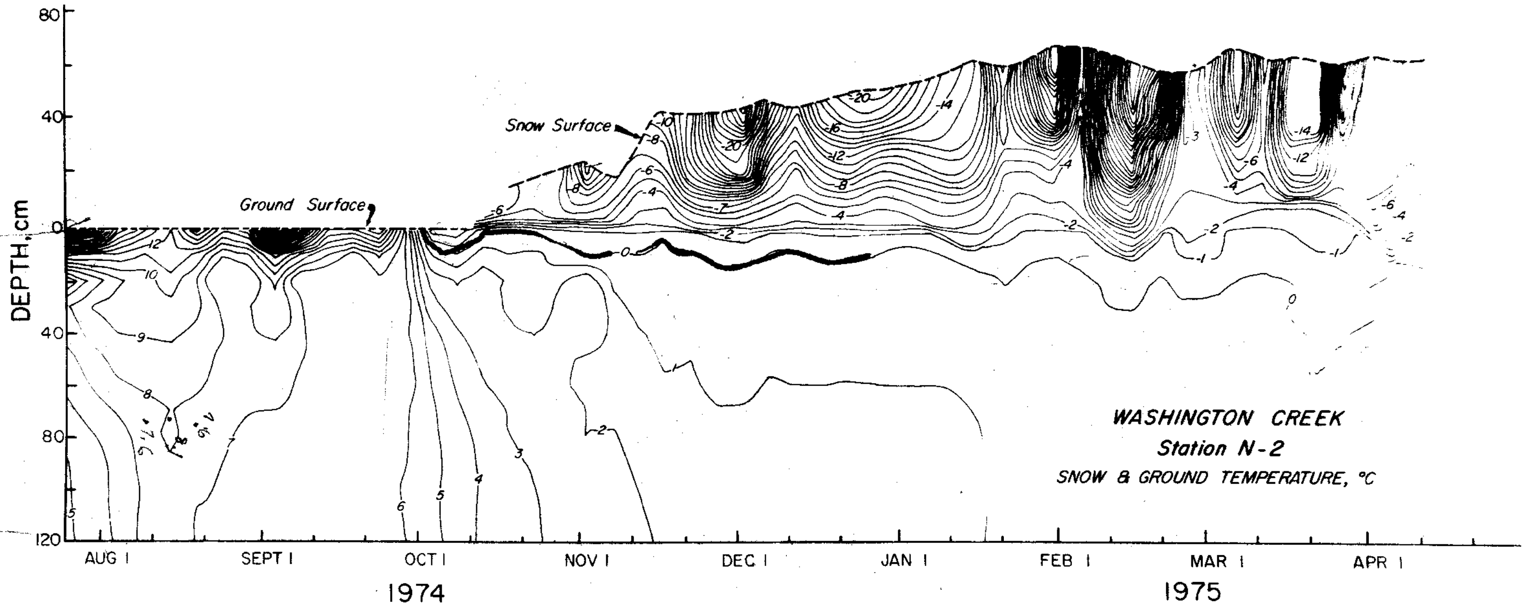

FIGURE 4: Ground and Snowpack Temperatures at Site N-2.

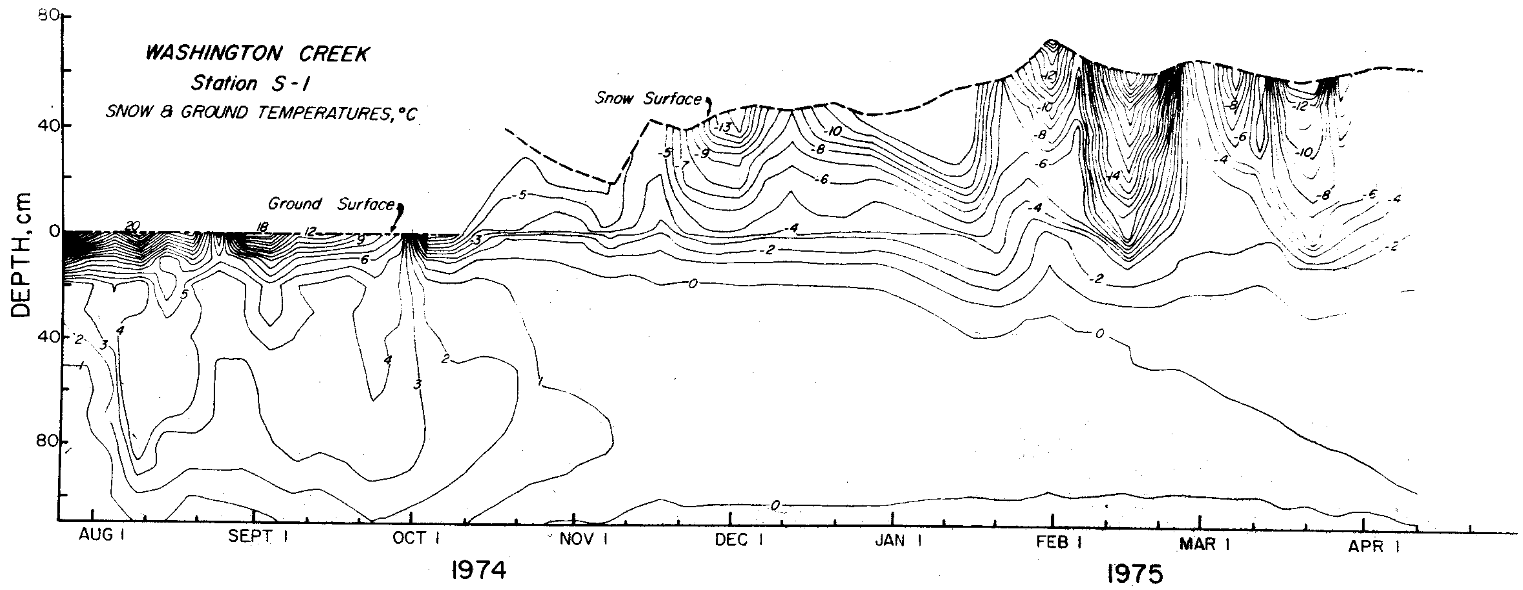

FIGURE 5: Ground and Snowpack Temperatures at Site S-1.

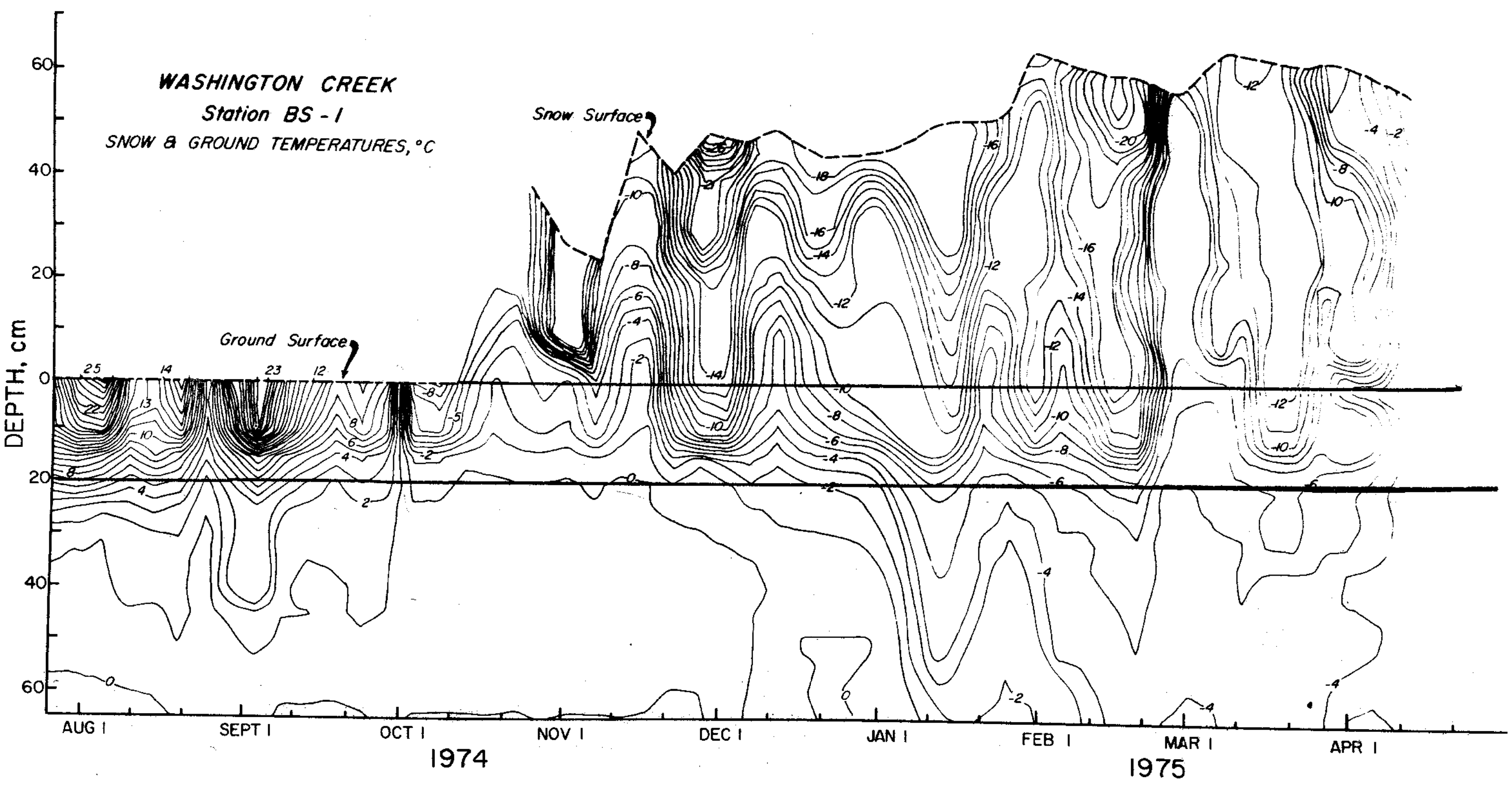

FIGURE 6: Ground and Snowpack Temperatures at Site BS-1.

at the lower unburned permafrost sites (BS-1, BS-2), 110 cm in the upper burned site adjacent to the burn (S-1, S-2) and no seasonal frost was detected in the burned area (N-1, N-2) at a depth of 120 cm. The insulative qualities of the organic layer are exhibited in both unburned sites; temperature in excess of 20°C were measured in these organic soils. Temperatures in the mineral soil of the unburned sites are comparable, even though the depth of thaw is much greater at the higher site. Temperatures throughout the mineral soil in the burn site were much warmer than at the two undisturbed sites.

Very rapid freeze-back of both the organic layer and mineral soil occurred at the unburned lower black spruce site during the early winter months. By the middle of December, the active layer had completely refrozen. At the other unburned site, it can be seen that the rate of freeze-back is much slower. The upward migration of the permafrost table can also be observed. Temperatures at the bottom of the active layer were measured at -4°C in the lower black spruce site and near 0°C in the upper black spruce sites. Between the 30 and 120 cm depth in the burned area, the temperatures were between 0 and 1°C. Measurements at depths greater than 120 cm in the burned area were hampered by broken schist fragments.

Troughs and ridges in the snow temperature contours reflect the winter ambient temperatures. Temperature measurements in the snowpack of the burned site and the lower unburned site were quite comparable. Temperatures in the higher unburned site along the ridge were several degrees warmer.

Pore Pressure Measurements

During late July, August, and early September, tensiometers filled with water were read 2 or 3 times per week (Figures 7 and 8). The soil tensions were lowest in the black spruce shallow permafrost setting (50-150 cm water), followed by the burned sites (75-225 cm water) and then the unburned deep permafrost site (100-300 cm of water). Measurement of soil tension in the organic layer was attempted, but it was very difficult to get meaningful

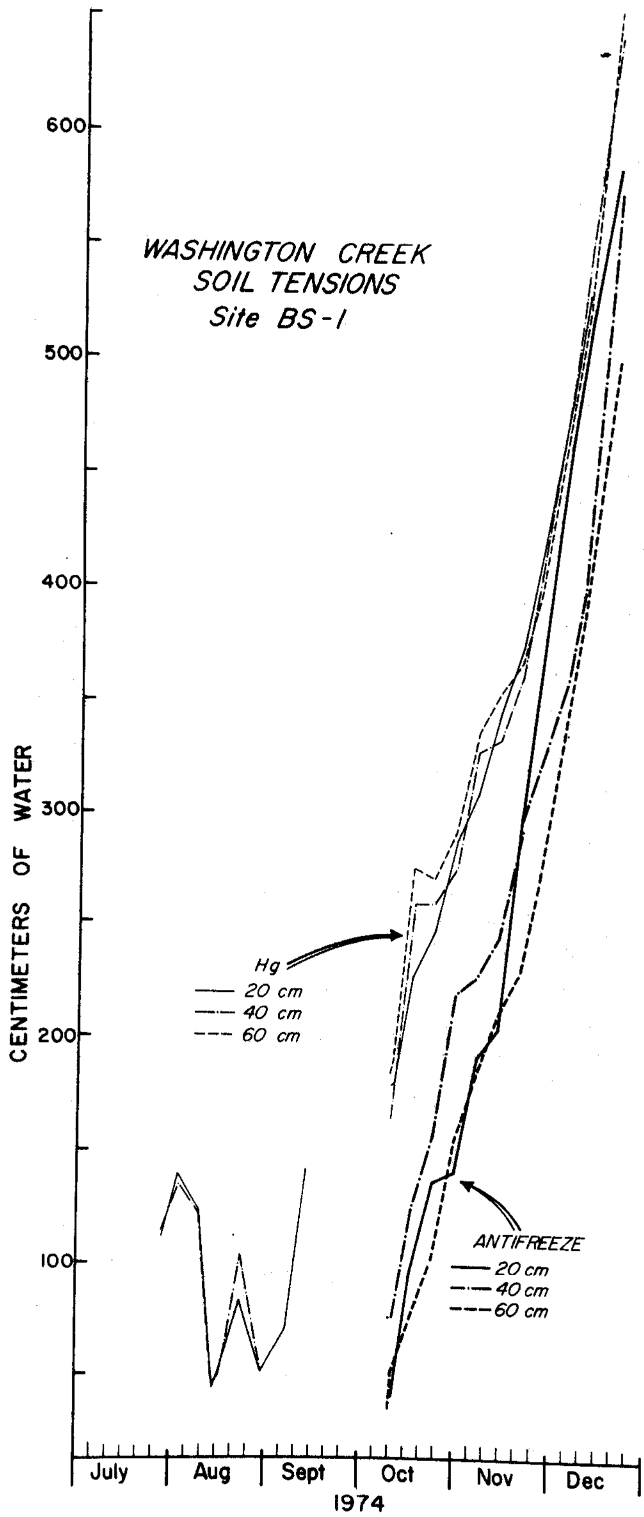

FIGURE 7: Measured Soil Tensions at Site BS-1.

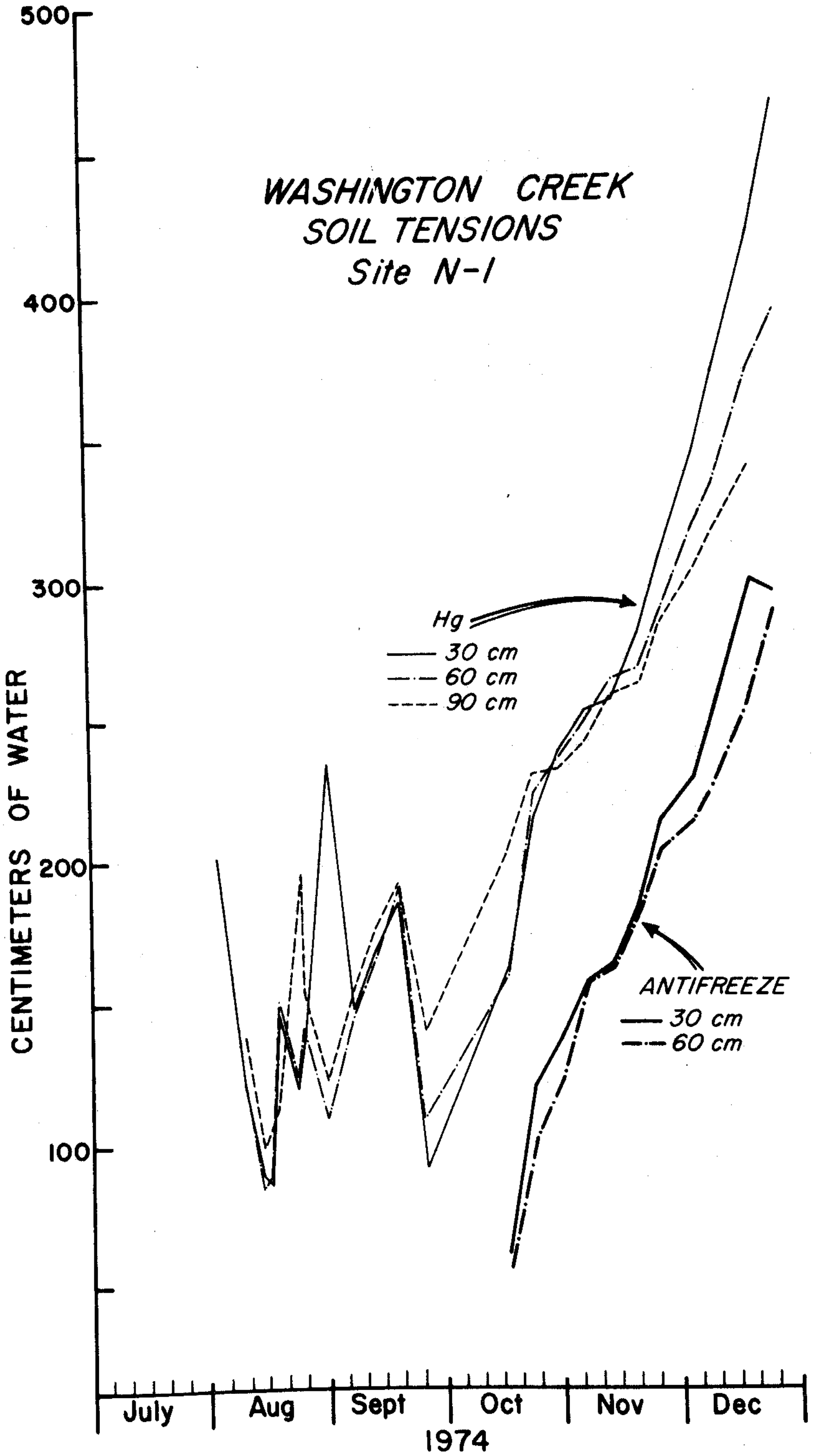

FIGURE 8: Measured Soil Tensions at Site N-1.

readings. It was apparent that this layer reacted very rapidly to surface cooling; negative pore pressures increased very rapidly, reflecting the loss of moisture.

The soil tension data during the summer at sites S-1, S-2, BS-2 and N-2 (Appendix B) have a very similar pattern. Examination of the precipitation graph and the soil tension curves show that soil tensions are low during and following periods of rainfall, steadily increase following this event, and continue to rise until the next event. Very sharp peaks were observed between August 20 and 30 at sites BS-2 and S-1. Both these tensiometers were in the organic layer and are showing a response to the first periods of frost. At this time, the soil temperatures at the surface were slightly below 0°C, while temperatures in the deeper soil layers were several degrees above freezing. The result of this colder temperature was to dry out the organic layer, as indicated by the high values of negative pore pressures.

This same trend is illustrated for the soil tension measurements made during the winter months. The tension values increased until the tensiometers failed during a very cold period in late December and early January. Values greater than 600 cm of H_2O and 450 cm of H_2O were measured respectively in the burned area and the black spruce site with shallow permafrost.

Soil Moisture Content

Soil samples were collected on a weekly basis at three sites for laboratory determination of moisture content. Once these soils froze, sampling on the two ridge sites was impossible with our available equipment due to rock fragments in the soil. However, the absence of such fragments at the lower black spruce site made it possible to collect data at approximate monthly intervals throughout the winter.

The soil moisture results verified the results from the tensiometers: the black spruce site with shallow permafrost was the wettest, followed by the burn site with the unburned ridge site being the driest.

On the following figures (9, 10, and 11) displaying soil moisture content, the moisture content is expressed as per cent by weight. Because of the variability of the bulk densities of the organic layer and mineral soil, it is advisable to represent the per cent moisture by volume. There is nearly an order of magnitude difference in moisture content when expressed as per cent by weight. Because of the format of the data, we have changed the contour interval.

The soil moisture content on each site, as well as between sites, shows a certain amount of fluctuation. These fluctuations can be due either to actual changes resulting from moisture fluxes or local variability. Because of local differences, little can be concluded about moisture content in the mineral soil. The maximum moisture content by weight is observed in the organic layer. There is far more change in the organic layer. Johnson (1964), in his study of the Hughes fire of 1962, discusses fuel types, particularly the lichen-moss complex, and states that the rate of moisture change within this fuel type was quite rapid. He indicates that it may lag behind changes in atmospheric moisture by less than one hour (of course this would depend upon the depth). He reports values of soil moisture content by weight of over 400% and less than 10%.

The general trend at the lower site (BS-1), which was monitored throughout the winter, was one of slow depletion of the soil moisture. This compares favorably with the upward migration of moisture as indicated by the tensiometer data. This movement would partially be in response to the thermal gradients that exist.

Hydrologic Modeling

Research specifically related to soil moisture dynamics in the subarctic and the effect of fire on the soil system is sparse. The first intense study of the temperature and moisture regime of a subarctic soil in Alaska was initiated and reported by Luthin and Guymon (1974). The measurements of pore pressure and temperatures were made in several vegetative systems. This work

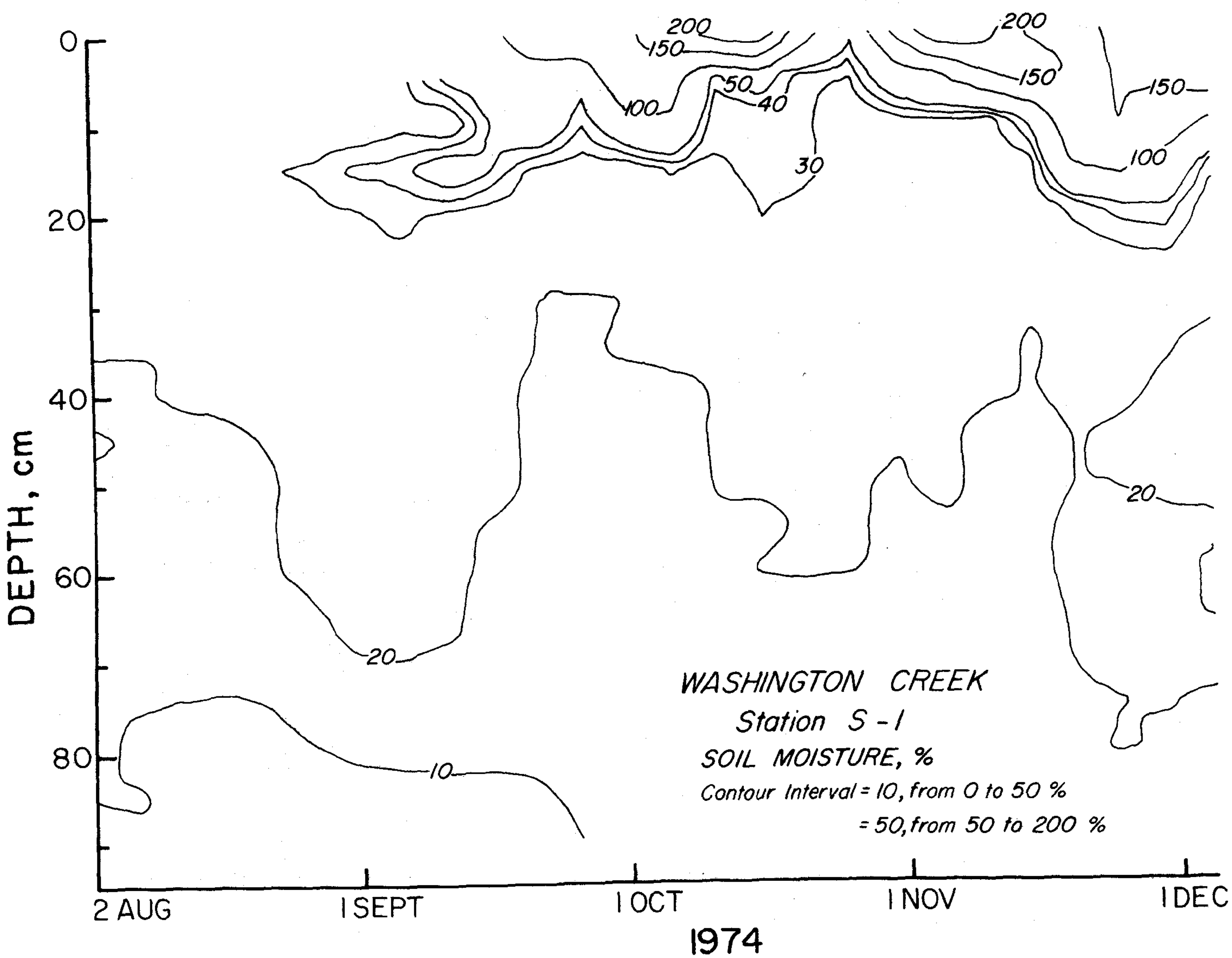

FIGURE 9: Soil Moisture Content, by Weight, at Site S-1.

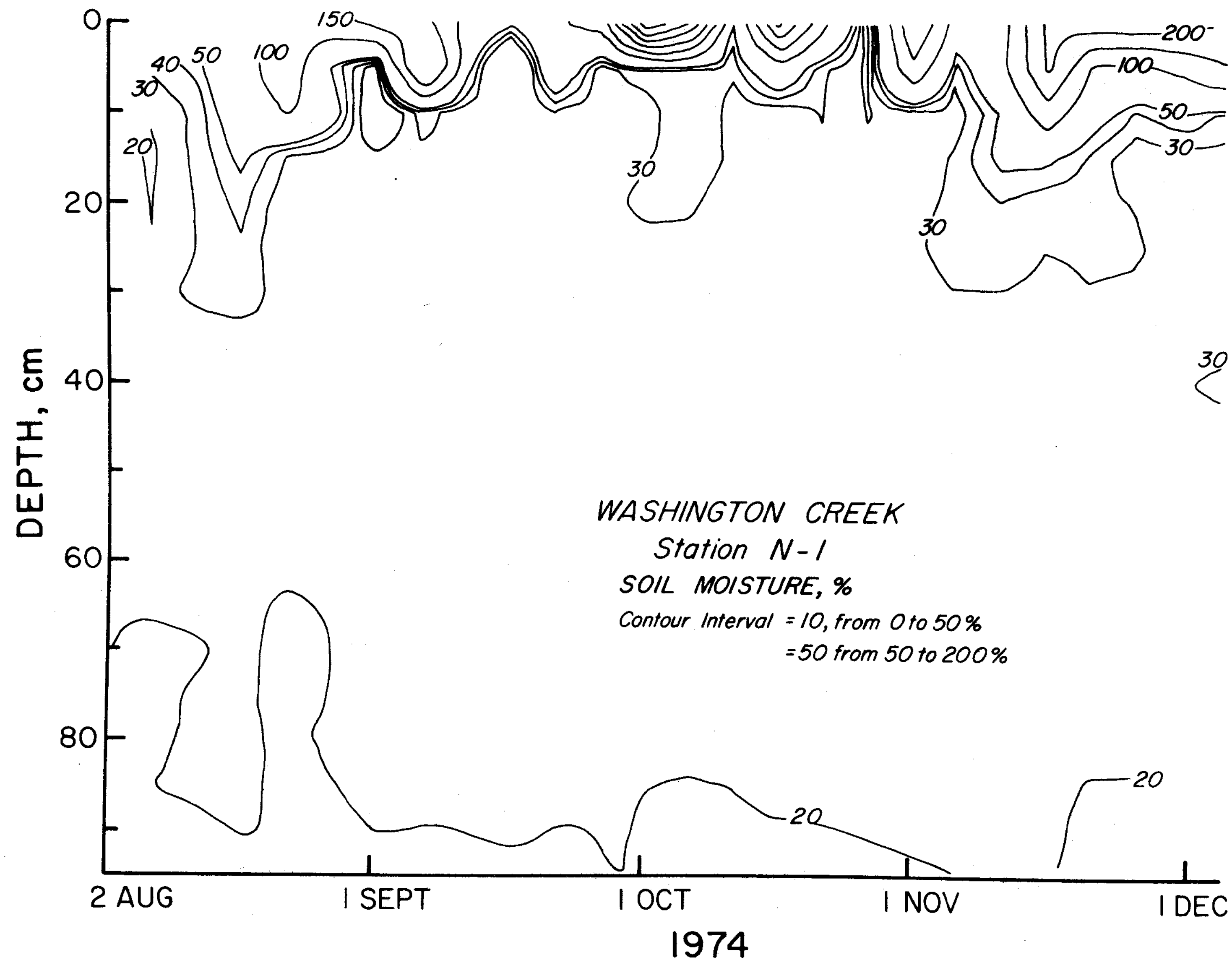

FIGURE 10: Soil Moisture Content, by Weight, at Site N-1.

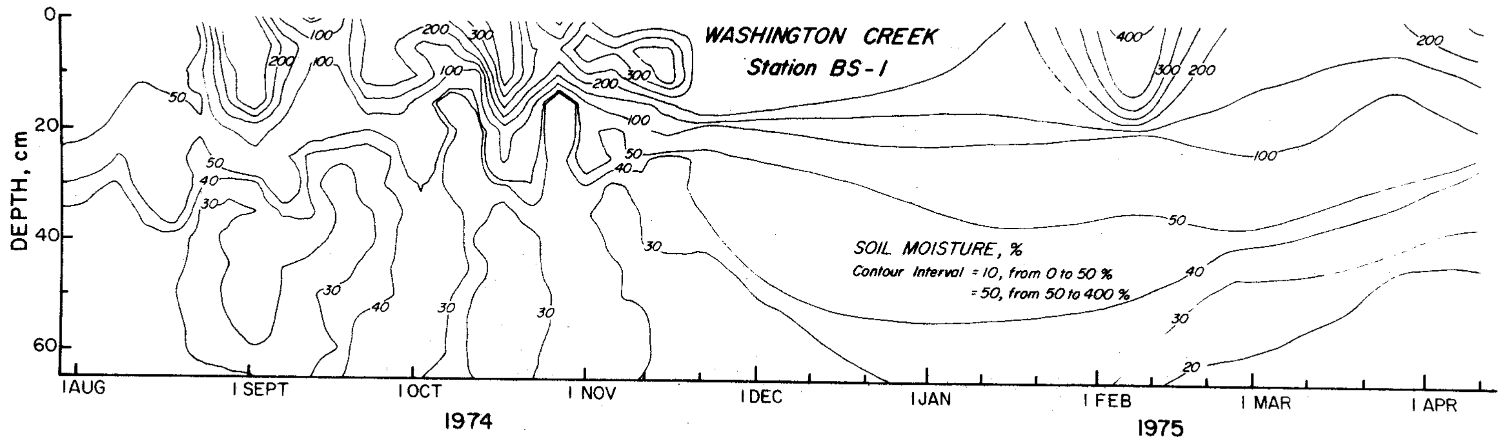

FIGURE 11: Soil Moisture Content, by Weight, at Site BS-1.

led to the development of a conceptual model relating drainage, vegetative cover, and the thermal regime of the mineral soil. An outgrowth of this project was a coupled heat and moisture transport model (Guymon and Luthin, 1974). Their work was primarily with mineral soil; however, as the study progressed, they recognized the importance of the surface organic layer.

Studies involving these same soils, when influenced by fires, are very limited. Viereck (1973) does an excellent job of detailing present hydrologically related work associated with wildfires in the taiga of Alaska. Most of the work reported in this paper deals with the thermal regime during the summer months. Studies related to the winter season and soil moisture status are lacking. The role of fire as an integral part of soil development is discussed by Pettapiece (1974) for a hummocky permafrost soil in northwestern Canada.

Because of the sparseness of data verifying coupled heat and moisture models and the need to further explore heat and moisture fluxes in the layered soils, particularly during winter, it was felt that a two-dimensional flow model would initially yield more useful information. One immediate application of this data would be the prediction of nutrient redistribution by soil water following a fire. To pursue this, a subsurface hydrologic model was developed to study water flow in these soils. The model is two-dimensional and simulates a flow region having uniform slopes of variable length and inclination. A highly permeable organic layer overlays the mineral soil. Because of its high porosity, the organic layer was given temporary water storage of 1.4 to 2.0 inches. At prescribed time intervals, rainfall or snow melt can be simulated. The resulting movement of water downslope was then evaluated in terms of hydrostatic pressure head, flow velocities, and moisture contents at different soil depths along the slope. The initial model simulated water movement following a single storm and for a given antecedent moisture condition. Subsequently, this model will be modified to simulate moisture movement throughout the hydrologic year. Available field and weather data will be utilized to estimate precipitation frequencies and amounts, depths of unfrozen soil and thickness and water transmission properties of the active soil layer. From these results, we can establish generalized patterns of water flow in these soils as affected by precipitation, slope, and organic layer characteristics.

The model is basically developed by utilizing the transient equation for liquid water transport in soil created by hydraulic gradients (Equation 2). This is the expression for Darcian-type flow in two-dimensional coordinates without sources and sinks. For saturated, porous media that is uniform and isotropic, this equation becomes the familiar Laplace-type expression. To solve Equation 2, experimental relationships between soil water content and pore water pressure head and those between soil hydraulic conductivity and pressure head are utilized.

A numerical analysis method is used in the solution of this partial differential equation. First we express the derivative terms in Equation 2 in finite difference form. The latter equation is then applied to each point in a two-dimensional grid that covers the flow region. These equations are then solved for pressure head H at various times t by the alternating-direction-implicit technique. The latter technique is essentially that reported by Douglas, Peaceman, and Rachford (1959) and Rubin (1968). The entire computing operation is programmed for an IBM 375/165 electronic computer.

In the analysis, we assume the mineral layer to be resting on an impermeable floor, the latter due to permafrost or impervious soil layer. Both organic and mineral layer can be characterized by experimental relationships among media water content, pressure head, and hydraulic conductivity. Estimated values for H are assigned initially to all grid points, then the resulting values are computed at t by solving Equation 2. A rainfall rate R can be simulated at the ground surface for specified time intervals. Water flow is evaluated following a single storm or snowmelt event and for a sequence of storms. The computed values of H will reveal time patterns of water content and flow velocities at various elevations and for different thicknesses and water-transmitting properties of the active layer:

$$\frac{\partial}{\partial x} K\frac{\partial(H+y)}{\partial x} + \frac{\partial}{\partial y} K\frac{\partial(H+y)}{\partial y} = S\frac{\partial H}{\partial t} \qquad (2)$$

where

$H = \frac{P}{\rho g}$ = the hydrostatic pressure head in the porous medium

P = the hydrostatic pressure

$(H+y)$ = the hydraulic head

K = the hydraulic conductivity of the medium. For negative values of H (i.e., capillary pressure head), K is a function of H

$S = \frac{\partial\theta}{\partial H}$ = the specific moisture capacity of the medium

θ = the water content of the medium expressed as a total volume fraction

x, y = the coordinate directions, y being parallel to the earth's gravitational field

ρ = mass fluid density

g = gravitational field strength

t = time

The two experimental relationships between soil water content and pore water pressure head and between hydraulic conductivity and pressure head used in the solution of the partial differential equation are:

$$K = K_o/(A_k H^3+1) \qquad (3)$$

$$\theta = \theta_o/(A_\theta H^3+1) \qquad (4)$$

where

K = unsaturated hydraulic conductivity

K_o = saturated hydraulic conductivity

θ = unsaturated soil moisture content

θ_o = moisture content under saturated conditions

A_k, A_θ = constants.

Use of these equations and proper selection of the constant A are discussed in a paper by Taylor and Luthin (1969). A plot of these relationships are shown in Figure 12 for A_k = .01 and A_θ = .001; these constants were selected for an organic soil with a saturated water content of 0.90 cm^3/cm^3 and a hydraulic conductivity of 50 cm/hour. These values of hydraulic conductivity and moisture content under saturated conditions are comparable to the values described by many researchers, particularly Dingman (1971) in his work on the Glenn Creek watershed just north of Fairbanks.

In this model the boundary conditions are presented as follows:

1. There was neglible water in the channel.
2. There was no moisture there across the lower boundary or the upslope vertical boundary.
3. No moisture existed across the surface boundary.

The stipulation that there is no moisture flux across the surface boundary is flexible. The program is written in order that fluxes can be handled across the boundary; however, because of the variability of this particular flux, it was felt that for the comparison of various cases, a simple approach would be used. Other than fluid and media properties, the two major variables of importance in any slope drainage problem are the dimensions and per cent slope. The variability of both of these features in natural settings is well appreciated. Due to the computer cost for each run, only a few runs with selected slope angles and slope lengths were made.

The output from this model is in tabular form with the position of the water table (saturated-unsaturated interface) indicated for various times by the calculated pore pressure. This information is plotted in Figure 13 for a slope of 20% and slope length of 8 m. It was assumed in this case that the slope was completelv saturated at time $t=0$. The drainage of this slope, once flow is initiated, is described by Equation 2. As may be seen in Figure 13, after 60 hours this slope is almost completely unsaturated. The length of time for complete drainage to occur depends directly on the slope length. It has been mentioned that there was not a flux across the upper vertical boundary, in the manner in which this figure is plotted, it appears that there is drainage across this boundary.

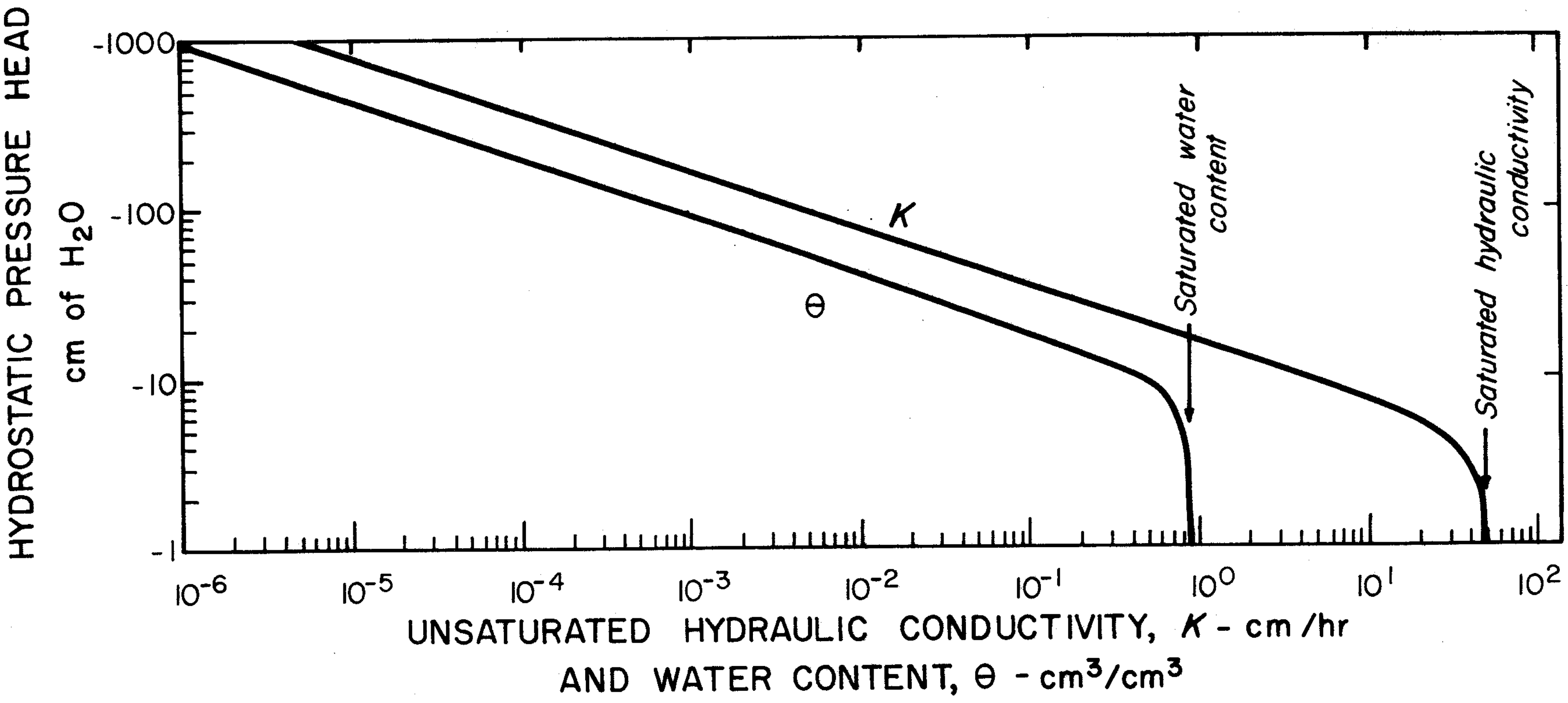

FIGURE 12: Hydraulic Conductivity and Water Content vs Hydrostatic Pressure Head.

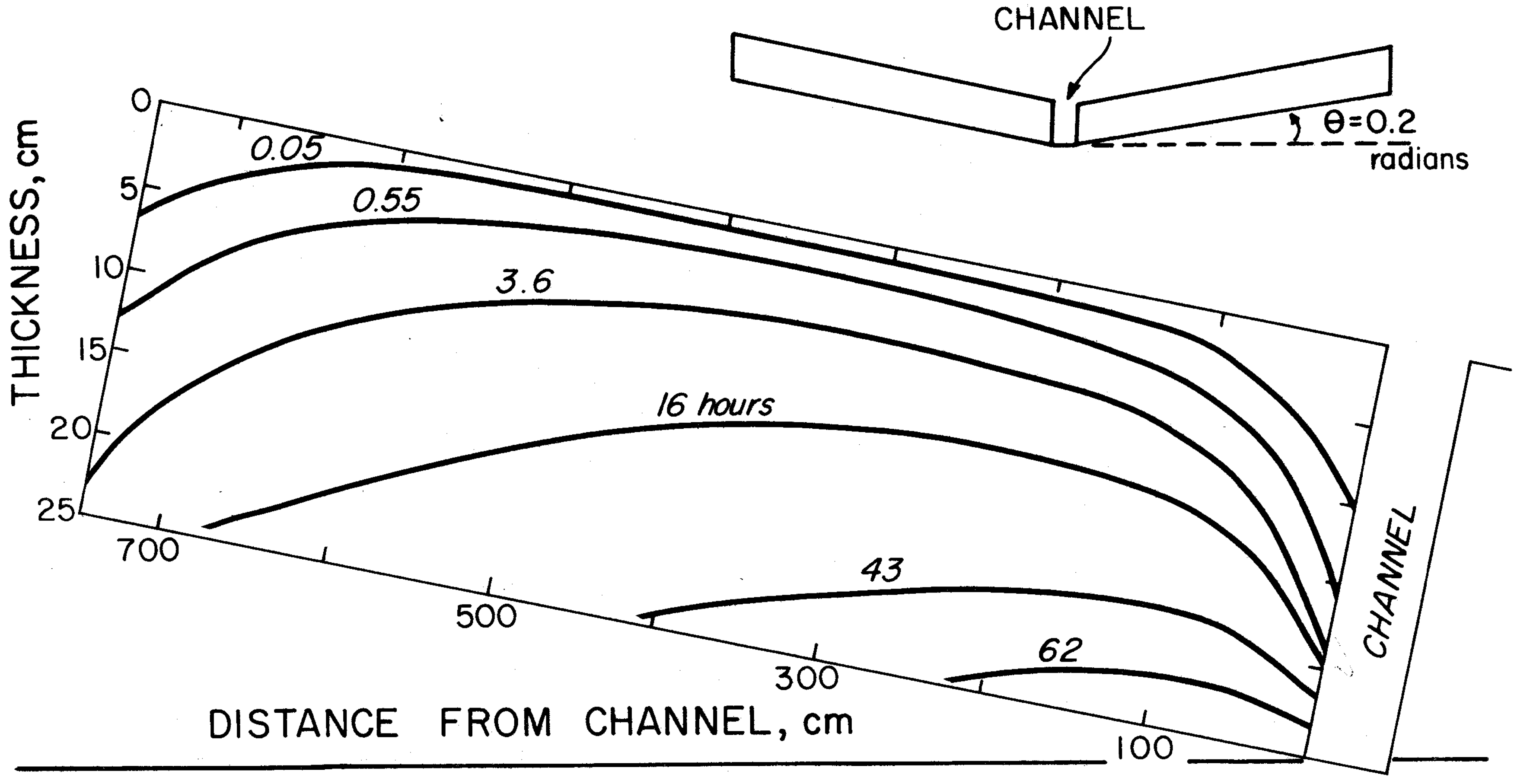

FIGURE 13: A Portion of a Water Table at Various Times in a Shallow Organic Soil under Natural Drainage, 8 m in Length and with a Slope of 20%.

Actually, all the flow is in the direction of the channel and, if this plot were drawn to scale, the lines indicating the water table conditions would slope toward the stream.

This model is also constructed in order that the flow regime of more than one layer can be computed. However, because of the layer variation in saturated hydraulic conductivity between organic soil and mineral soil, we restricted ourselves to the organic layer where the greatest changes occur.

From the previous results, the outflow rate in cm^3/cm/hour can be determined. The flow rate for various slope lengths is shown (Figure 14), for a 20% slope and a saturated hydraulic conductivity of 50 cm/hour. Curves for other initial moisture contents could be generated, providing curves for more realistic conditions.

CONCLUSIONS

The recognition that many beneficial effects of fire do occur has altered the present fire control philosophy. From our field data, it is clear that both the thermal and moisture regimes undergo considerable alterations because of fires. The degree to which these systems are influenced depends upon many factors, primarily the intensity of the burn. Prior to any fire, natural variations occur because of slope, aspect, and vegetation and soil conditions. Basically, fires tend to add more variability to the natural setting.

It is this variability that makes modeling on a watershed scale very difficult. Alteration of the system will have to be linked with the intensity of the burn. Assuming acceptable models are generated and prescribed burning becomes a reality, models for predicting the fire intensity beforehand will have to be developed. These models will be based on weather and fuel conditions prior to and during the fire, as well as terrain features.

The conclusions reached from the temperature and soil moisture data are:

1. That thermal regime is substantially altered by fire; it appears that the conceptual model presented accurately defines the long range

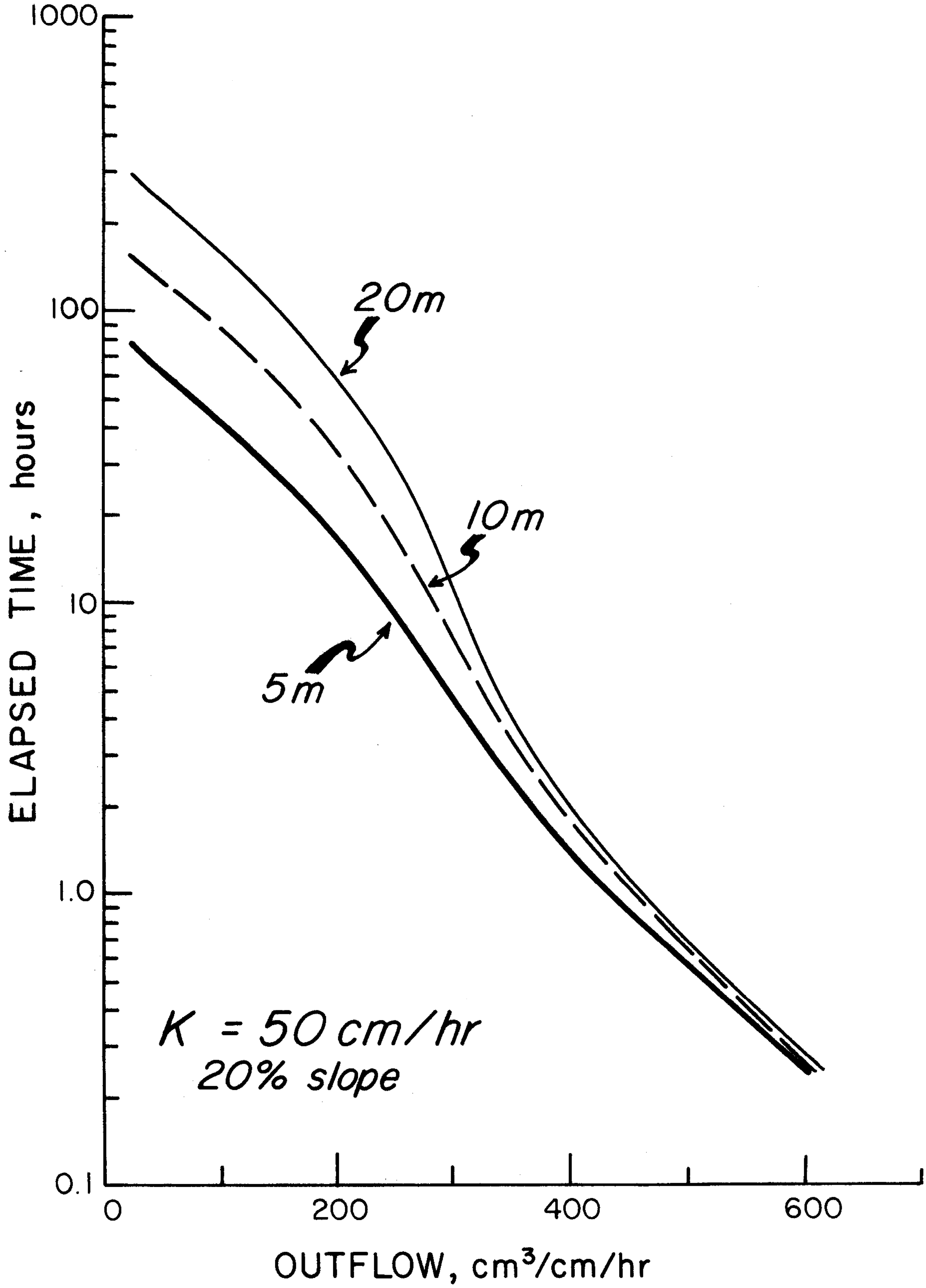

FIGURE 14: A Plot of the Outflow Rate for Different Slope Lengths Following the Initiation of Drainage.

pattern of the thermal regime. It is apparent from the field data that temperatures in the burned area are much higher than those in the unburned area for both summer and winter seasons. The variation in the thermal regimes of the two unburned sites is not as apparent. It should be emphasized that the difference in the depth to the permafrost table differs almost by a factor of 2. This represents the magnitude of variance expected due to differences in vegetation, slope, slope aspect, drainage, etc. The depth to the permafrost table in the burned area was never determined. From the measured temperatures, it is clear that it is now at a depth of several meters (and degrading); prior to the burn, it was probably at a depth near 1 meter.

2. The near-surface moisture regime is influenced by fire, but not to the same degree as the thermal regime. Due to a decrease in evapotranspiration losses, the total moisture content in a column of soil should increase. This is obvious from our data; however, the natural variability that exists in undisturbed areas exceeds our observed variability between an unburned site and a burned site. One reason for this observation is that where permafrost exists, the water is confined to a thin layer near the surface. As the permafrost degrades however, there is a much thicker near-surface layer in which this water may be retained or through which it may be transmitted. The role of the organic layer in a burned environment depends upon the intensity of the fire. In organic soils in unburned settings, the tensiometer data shows that water is retained by this layer and later lost by evapotranspiration. It would be expected that saturated conditions would develop only during heavy rains. This would result in a lateral flow as well as an addition of water to the lower mineral soil. The tensiometer data for early winter reveals that the movement of soil moisture is upward towards the surface, resulting in some depletion in both the organic and mineral layers. The part played by heat conduction in thawing frozen soils is well understood; however, the amount of heat transmitted by convection (flowing water) above or through a frozen soil is not known.

3. The flow results from the computer model give some insight into the length of time associated with drainage of the organic layer and the rate of outflow from a slope of given width. During the period in which the summer field data was collected, rainfall was exceedingly light and was never sufficient to produce saturated conditions in the organic layer. Dingman (1971) reports that the water-holding capacity of organic soils and the moisture content that we measured was nearly 400% by weight. Since the conditions necessary to cause lateral flow never occurred, no comparison with theoretical results is possible.

A multitude of problems need to be researched before the capability to predict changes resulting from fire in major ecosystems processes is possible. We have touched only one aspect of the system.

REFERENCES

Barney, R. J. (1971). Wildfires in Alaska - some historical and projected effects and aspects. Proceedings: *Fire in the Northern Environment*, Fairbanks, Alaska, April 13-14, 1971, pp. 51-59.

Dingman, S.L. (1971). Hydrology of the Glenn Creek watershed, Tanana River Basin, Central Alaska. U.S. Army Cold Regions Research and Engineering Laboratory, Research Report 297.

Douglas, J. D.; Peaceman, W.; and Rachford, H. H. (1959). A method for calculating multi-dimensional immiscible displacement. *Amer. Inst. Mining, Met. & Petrol. Eng.*, Trans. 216:297-308.

Furbush, C. E., and Schoeporster, D. B. (1974). Soils of the Wickersham Dome Experimental Forest, Alaska. U.S. Department of Agriculture, Soil Conservation Service.

Guymon, G. L., and Luthin, J. N. (1974). A coupled heat and mass transport model for Arctic soils. *Water Resources Research*, Vol. 10, No. 5, pp. 995-1001.

Johnson, V. S. (1964). The Chronology and Analysis of the Hughes Fire, 1962. U.S. Dept. of Agriculture, Forest Service, Research Not NOR-8.

Lee, R. (1962). Theory of equivalent slope. *Monthly Weather Review*, Vol. 90, pp. 165-166.

Luthin, J. N., and Guymon, G. L. (1974). Soil moisture - vegetation - temperature relationships in central Alaska. *Journal of Hydrology*, Vol. 23, pp. 233-246.

Miller, R. S.; Smith, R. B.; and Biggar, J. W. (1974). Soil water content: microwave oven method. *Soil Science Society of America Proceedings*, Vol. 38, pp. 535-537.

Pettapiece, W. W. (1974). A Hummocky Permafrost Soil from the Subarctic of Northwestern Canada and Some Influences of Fire. *Canadian Journal of Soil Sciences*, Vol. 54, pp. 343-355.

Plamondon, P. A.; Black, T. A.; and Goodell, B. C. (1972). The Role of Hydrologic Properties of the Forest Floor in Watershed Hydrology, National Symposium on Watersheds in Transition. American Water Resources Association, Ft. Collins, Colorado, June 19-22, 1972, pp. 341-348.

Rubin, J. (1968). Theoretical analysis of two-dimensional transient flow of water in unsaturated and partly-saturated soils. *Soil Sci. Amer. Proc. 32:*607-615.

Taylor, G. S., and Luthin, J. N. (1969). Computer methods for transient analysis of water table aquifers. *Water Resources Research*, Vol. 5, No. 1, pp. 144-152.

Viereck, L. A. (1973). Wildfire in the taiga of Alaska. *Quaternary Research*, Vol. 3, pp. 465-495.

Williams, P. J., and Burt, T. P. (1974). Measurement of hydraulic conductivity of frozen soils. *Canadian Geotechnical Journal*, Vol. 11, pp. 647-650.

APPENDIX A

COMPUTER MODEL

```
C   TAYLOR.1975,TWO-LAYERED MEDIUM,TRANSIENT FLOW ON SLOPING COLD REGION SOILS
      DIMENSION D(12,34,2),W(12,34,3),S(12,34,3),B(34),G(34),R(34)
   10 FORMAT(7I10)
   15 FORMAT(4X,9I4)
   16 FORMAT (7E10.3)
   17 FORMAT(4X,2I3,F15.5)
   20 FORMAT(7F10.5)
   25  FORMAT (/,10E11.3)
   30 FORMAT (/,16F7.2)
   35 FORMAT (/,16F7.0)
   40 FORMAT(2X,'TOTAL ITERATIONS=',I4,2X,'LAST ITERATION SET=',I2,
     12X,'NO. WATER CONTENT CHANGES=',I3,2X,4I5)
   41 FORMAT (2X,'TIME INCREMENT=',E9.3,2X,'TOTAL TIME ELAPSED=',
     1E9.3,2X,'ERROR=',F7.3)
   42 FORMAT (/,16F7.1)
   44 FORMAT (/,16F7.4)
      READ (5,10) M,N,INT,ITN3,ITN4,ITN6,ITN8
      READ (5,10) ITER,K1,K2,K3,K4,K5,K6
      N1=N-1
      N2=N-2
      M1=M-1
      M3=M+1
      M2=M-2
      I6=INT-1
      READ(5,20) A,B1,DELT,RAD,ERR,C1,C2
      READ (5,20) C3,C4,C5,C6,C7,C8,C9
      READ (5,20) T,T3,T4,BOK,TIME,SLOPE
      READ (5,16) C10,C11,C12,C13,C14,C15,C16
      READ(5,20) (R(J),J=1,N)
      WRITE (6,10) M,N,INT,ITN3,ITN4,ITN6,ITN8
      WRITE (6,10) ITER,K1,K2,K3,K4,K5,K6
      WRITE(6,20) A,B1,DELT,RAD,ERR,C1,C2
      WRITE(6,20) C3,C4,C5,C6,C7,C8,C9
      WRITE (6,20) T,T3,T4,BOK,TIME,SLOPE
      WRITE (6,16) C10,C11,C12,C13,C14,C15,C16
      WRITE(6,35) (R(J),J=1,N)
      THETA=ATAN(SLOPE)
      C17=C2/4.
      C18=C2
C C17 AND C18 CONTROL C2
C    SETTING INITIAL CONDITIONS
      DO 80 J=1,N
      DO 80 I=2,M
      X=I-2
      XX=M-I
      W(I,J,1) =A*XX
      IF (I.NE.M) GO TO 68
      W(M,J,1) = -0.5
   68 IF(J.NE.N) GO TO 70
      W(I,N,1)=0.0
      W(M,N,1)= -1.
   70 IF (I.EQ.3) W(1,J,1)=W(3,J,1)+2.*A*COS(THETA)
      IF (I.EQ.M) W(M3,J,1)=W(M1,J,1)-2.*A*COS(THETA)
      IF (W(I,J,1).GE.0.0) GO TO 76
      IF (I.LT.INT) GO TO 72
      S(I,J,1)=3.0*0.90*C11*W(I,J,1)**2/(C11*ABS(W(I,J,1))**3+1.0)**2
      IF (S(I,J,1).LT.0.001) S(I,J,1)=.001
      D(I,J,1)=C4*(C13*ABS(W(I,J,1))**3+1.0)
```

```
      IF (I.NE.INT) GO TO 78
      S(1,J,1)=3.0*0.45*C12*W(INT,J,1)**2/(C12*ABS(W(INT,J,1))
     1**3+1.0)**2
      IF (S(1,J,1).LT.0.001) S(1,J,1)=.001
      S(1,J,2)=S(1,J,1)
      D(1,J,1)=C5*(C14*ABS(W(INT,J,1))**3+1.0)
      D(1,J,2)=D(1,J,1)
      GO TO 78
   72 S(I,J,1)=3.0*0.45*C12*W(I,J,1)**2/(C12*ABS(W(I,J,1))**3+1.0)**2
      IF (S(I,J,1).LT.0.001) S(I,J,1)=0.001
      D(I,J,1)=C5*(C14*ABS(W(I,J,1))**3+1.0)
      GO TO 78
   76 S(I,J,1)=0.0
      IF (I.EQ.INT) D(1,J,1)=C5
      D(I,J,1)=C4
      IF (I.LT.INT) D(I,J,1)=C5
   78 W(I,J,2)=W(I,J,1)
      W(I,J,3)=W(I,J,1)
      S(I,J,2)=S(I,J,1)
      D(I,J,2)=D(I,J,1)
      D(M3,J,1)=D(M1,J,1)
      D(M3,J,2)=D(M1,J,1)
      D(I,1,1)=D(I,3,1)
      D(I,1,2)=D(I,3,1)
      IF (INT.LT.2) D(1,J,1)=D(3,J,1)
      IF (INT.LT.2) D(1,J,2)=D(3,J,1)
      IF (INT.LT.2) S(1,J,1)= S(3,J,1)
      IF (INT.LT.2) S(1,J,2)=S(3,J,1)
      W(1,J,2)=W(1,J,1)
      W(1,J,3)=W(1,J,1)
      W(M3,J,3)=W(M3,J,1)
      W(1,1,3)=W(1,1,1)
      W(M3,J,2)=W(M3,J,1)
   80 CONTINUE
      DO 90 K=1,M1
      I=M3-K
   90 WRITE (6,30) (W(I,J,1),J=2,N,K3)
C     HYDROSTATIC PRESSURE IMPLICIT IN X-DIRECTION
  150 ITER=ITER+1
      ITN6=ITN6+1
      T3=T3+T4
      I=1
      IF(T3.LE.C6) GO TO 154
      T3=C6
  154 I=I+1
      IF (I.GT.M) GO TO 322
      C=R(2)-R(1)
  160 DO 300 J=2,N1
      E=R(J+1)-R(J)
      DELV=A*(C+E)/2.0
      XI=A/(2.0*(C+E))
      DD=D(I,J,1)+D(I,J,2)
      D1=D(I+1,J,1)+D(I+1,J,2)
      D3=D(I-1,J,1)+D(I-1,J,2)
      D10=(DD+D(I,J+1,1)+D(I,J+1,2))/2.
      IF (I.EQ.M) GO TO 174
      D11=(D1+D(I+1,J+1,1)+D(I+1,J+1,2))/2.
      IF (I.NE.I6) GO TO 164
```

```
      D1=D(1,J,1)+D(1,J,2)
      D11=(D1+D(1,J+1,1)+D(1,J+1,2))/2.
  164 X11=ABS(ALOG(D11/D10))
      X12=ALOG(D11/D10)
      IF (X11.GT.0.693) GO TO 168
      R22=(D10+D11)*E/(2.0*A)
      GO TO 170
  168 R22=E*D10*X12/(A*(1.0-EXP(-X12)))
  170 X11=ABS(ALOG(D1/DD))
      X12=ALOG(D1/DD)
      IF (X11.GT.0.693) GO TO 172
      R1=(DD+D1)*X1
      GO TO 174
  172 R1=A*DD*(EXP(X12)-1.0)/(X12*(C+E))
  174 D13=(D3+D(I-1,J+1,1)+D(I-1,J+1,2))/2.
      IF (I.NE.INT) GO TO 176
      DD=D(1,J,1)+D(1,J,2)
      D10=(DD+D(1,J+1,1)+D(1,J+1,2))/2.
  176 X11=ABS(ALOG(D10/D13))
      X12=ALOG(D10/D13)
      IF (X11.GT.0.693) GO TO 178
      R222=(D10+D13)*E/(2.0*A)
      GO TO 180
  178 R222=E*D13*X12/(A*(1.0-EXP(-X12)))
  180 X11=ABS(ALOG(DD/D3))
      X12=ALOG(DD/D3)
      IF (X11.GT.0.693) GO TO 182
      R3=(DD+D3)*X1
      GO TO 184
  182 R3=A*D3*(EXP(X12)-1.0)/(X12*(C+E))
      X14=EXP(X12)
  184 IF (1.EQ.M) R22=R222
      IF (I.EQ.2) R222=R22
      R2= R22*R222/(R22+R222)
      IF (J.EQ.2) R4=R2
      IF (I.EQ.2) R3=R1
      IF (I.EQ.M) R1=R3
      DAG=1.0/D(I,J,1)
      IF (I.EQ.INT) DAG=(DAG+1.0/D(1,J,1))/2.0
      DAG=(T**T3)*DAG
      F24=DELV*(S(1,J,1)+S(I,J,2))/(2.0*DELT)
      IF (I.EQ.INT) F24=DELV*(S(I,J,1)+S(1,J,1))/(2.0*DELT)
      ALF=1.0/R4
      CEE=1.0/R2
      FRAG3=1/R3
      FRAG2=1/R1
      BET=-(ALF+CEE+F24+DAG)
      FRAG=FRAG3+FRAG2-DAG
      DOG=-FRAG3*W(I-1,J,3)-FRAG2* W(I+1,J,3)+FRAG*W(I,J,3)+A*
     1COS(THETA)*(FRAG3-FRAG2)+SIN(THETA)*(E*CEE-C*ALF)-F24*W(I,J,1)
      IF (1.EQ.M) DOG=DOG-BOK*(R(J+1)-R(J-1))*COS(THETA)/2.0
  186 IF (J.EQ.2) GO TO 220
      IF (J.EQ.N1) GO TO 225
      DENOM=BET+ALF*G(J-1)
      B(J)=(DOG-ALF*B(J-1))/DENOM
      G(J)=-CEE/DENOM
      GO TO 230
  220 DOG=DOG+2.0*(R(3)-R(2))*SIN(THETA)*CEE
```

```
      B(2)=DOG/BET
      G(2)=-2.0*CEE/BET
      GO TO 230
  225 X=W(I,N1,2)
      W(I,N1,2)=(DOG-CEE*W(I,N,1)-ALF*B(N2))/(ALF*G(N2)+BET)
  227 IF (ITN6.LT.15) GO TO 230
      XX=ABS(ABS(W(I,N1,2))-ABS(X))
      IF (XX.LT.C3) GO TO 230
      W(1,N1,2)=(W(1,N1,2)+X)/2.0
  230 C=E
  235 R4=R2
  300 CONTINUE
C     SETTING VALUES OF H IN X-DIRECTION
  310 DO 320 K=2,N2
      J=N1-K+1
      X=W(I,J,2)
      W(I,J,2)=B(J)+G(J)*W(I,J+1,2)
  315 IF (ITN6.LT.15) GO TO 320
      XX=ABS(ABS(W(I,J,2))-ABS(X))
      IF (XX.LT.C3) GO TO 320
      W(1,J,2)=(W(1,J,2)+X)/2.0
  320 CONTINUE
      W(I,1,2)=W(I,3,2)-2.0*(R(3)-R(2))*SIN(THETA)
      GO TO 154
  322 DO 340 J=1,N
      W(1,J,2)=W(3,J,2)+2.0*A*COS(THETA)
  340 W(M3,J,2)=W(M1,J,2)-2.0*A*COS(THETA)
      ERROR=0.0
      IF (ITN4.GE.0) GO TO 400
      DO 360 K=1,M3
      I=M3-K+1
  360 WRITE (6,30) (W(I,J,2),J=1,N,K3)
  400 J=1
C     HYDROSTATIC PRESSURE IMPLICIT IN Y-DIRECTION
      C=R(3)-R(2)
  403 J=J+1
      IF (J.GT.N1) GO TO 530
      E=R(J+1)-R(J)
      DELV=A*(C+E)/2.0
      X1=A/(2.0*(C+E))
      DO 500 I=2,M
      DD=D(I,J,1)+D(I,J,2)
      D1=D(I+1,J,1)+D(I+1,J,2)
      D10=(DD+D(I,J+1,1)+D(I,J+1,2))/2.
      D11=(D1+D(I+1,J+1,1)+D(I+1,J+1,2))/2.
      D20=(DD+D(I,J-1,1)+D(I,J-1,2))/2.0
      D22=(D1+D(I+1,J-1,1)+D(I+1,J-1,2))/2.0
      IF (I.NE.I6) GO TO 405
      D1=D(1,J,1)+D(1,J,2)
      D11=(D1+D(1,J+1,1)+D(1,J+1,2))/2.
      D22=(D1+D(1,J-1,1)+D(1,J-1,2))/2.
  405 IF (I.EQ.M) GO TO 418
      X11=ABS(ALOG(D11/D10))
      X12=ALOG(D11/D10)
      IF (X11.GT.0.693) GO TO 408
      R22=(D10+D11)*E/(2.0*A)
      GO TO 410
  408 R22=E*D10*X12/(A*(1.0-EXP(-X12)))
```

```
  410 X11=ABS(ALOG(D1/DD))
      X12=ALOG(D1/DD)
      IF (X11.GT.0.693) GO TO 412
      R1=(DD+D1)*X1
      GO TO 414
  412 R1=A*DD*(EXP(X12)-1.0)/(X12*(C+E))
  414 IF (J.EQ.2) GO TO 418
      X11=ABS(ALOG(D22/D20))
      X12=ALOG(D22/D20)
      IF (X11.GT.0.693) GO TO 416
      R44=(D20+D22)*C/(2.0*A)
      GO TO 418
  416 R44=C*D20*X12/(A*(1.0-EXP(-X12)))
  418 IF (I.EQ.M) R22=R222
      IF (I.EQ.M) R44=R444
      IF (I.EQ.2) R444=R44
      IF (I.EQ.2) R222=R22
      R2=R22*R222/(R22+R222)
       IF (J.EQ.2) GO TO 420
      R4=R44*R444/(R44+R444)
  420 IF (I.EQ.2) R3=R1
      IF (I.EQ.M) R1=R3
      IF (J.EQ.2) R4=R2
      DAG=1./D(I,J,1)
      IF (I.EQ.INT) DAG=(DAG+1.0/D(1,J,1))/2.0
      DAG=(T**T3)*DAG
      ALF=1.0/R3
      CEE=1.0/R1
      F24=DELV*(S(I,J,1)+S(I,J,2))/(2.0*DELT)
      BET=-(ALF+CEE+F24+DAG)
      FRAG3=1.0/R4
      FRAG2=1.0/R2
      FRAG=(FRAG3+FRAG2-DAG)
      DOG=-FRAG3*W(I,J-1,2)-FRAG2*W(I,J+1,2)+FRAG*W(I,J,2)+A*
     1COS(THETA)*(ALF-CEE)+SIN(THETA)*(E*FRAG2-C*FRAG3)-F24*W(I,J,1)
      IF (I.EQ.M) DOG=DOG-BOK*(R(J+1)-R(J-1))*COS(THETA)/2.0
  422 IF(I.NE.2) GO TO 455
      B(2)=(DOG-2.0*CEE*A*COS(THETA))/BET
      G(2)=-2.0*CEE/BET
      GO TO 475
  455 IF (I.EQ.M) GO TO 465
      DENOM=(BET+ALF*G(I-1))
      B(I)=(DOG-ALF*B(I-1))/DENOM
      G(I)=-CEE/DENOM
      GO TO 475
  465 X=W(M,J,3)
      W(M,J,3)=(DOG+2.*A*ALF*COS(THETA)-2.*ALF*B(M1))/(2.*ALF*G(M1)+BET)
  470 IF (ITN6.LT.15) GO TO 475
      XX=ABS(ABS(W(M,J,3))-ABS(X))
      IF (XX.LT.C3) GO TO 475
      W(M,J,3)=(W(M,J,3)+X)/2.0
  475 R444=R44
  476 IF(ITN3.LT. 9)GO TO 497
      IF(T3.LT.C6)GO TO 497
      IF(I.NE.2) GO TO 477
      S(2,J,3) = (W(I,J,3) - W(I,J+1,3) + E*SIN(THETA))*2./R22
      GO TO 497
  477 S(1,J,3)= S(I-1,J,3) + (W(I,J,3)-W(I,J+1,3)+E*SIN(THETA))*2./R22
```

```
  497 R3=R1
      R222=R22
  500 CONTINUE
      DO 510 K=1,M2
      I=M-K
      X1=W(I,J,3)
      W(I,J,3)=B(I)+G(I)*W(I+1,J,3)
  505 Y=ABS(ABS(W(I,J,3))-ABS(X1))
      IF (Y.GT.C3) ERROR=ERROR+1.0
      IF (ITN6.LT.15) GO TO 510
      IF (Y.LT.C3) GO TO 510
      W(I,J,3)=(W(I,J,3)+X1)/2.0
  510 CONTINUE
      W(1,J,3)=W(3,J,3)+2.0*A*COS(THETA)
      W(M3,J,3)=W(M1,J,3)-2.0*A*COS(THETA)
      C=E
      GO TO 403
  530 DO 540 I=1,M3
      W(I,1,3)=W(I,3,3)-2.0*(R(3)-R(2))*SIN(THETA)
  540 CONTINUE
      IF (ITN4.GE.0) GO TO 543
      DO 542 K=1,M3
      I=M3-K+1
  542 WRITE (6,30) (W(I,J,3),J=1,N,K3)
  543 K7=0
      K8=0
      K9=0
      DO 560 J=2,N
      DO 560 I=2,M
      IF (T3.LT.C6) GO TO 554
      IF (ITN6.GE.K2) GO TO 544
      IF (ERROR.GT.2) GO TO 554
  544 X=W(I,J,1)
  546 XX=ABS(ABS(W(I,J,3))-ABS(X))
      IF (XX.LT.C2) K8=K8+1
      IF (XX.GT.C2) K9=K9+1
      X1X=C2*1.1
      IF (XX.GT.X1X) K7=K7+1
      W(I,J,1)=W(I,J,3)
      IF (I.NE.2) GO TO 548
      W(1,J,1)=W(1,J,3)
      W(M3,J,1)=W(M3,J,3)
  548 IF (J.NE.2) GO TO 550
      W(I,1,1)=W(I,1,3)
  550 IF (J.EQ.N) GO TO 552
      W(I,J,3)=2.0*W(I,J,3)-X
  552 W(M3,J,3)=W(M1,J,3)-2.*A*COS(THETA)
      W(1,J,3)=W(3,J,3)+2.*A*COS(THETA)
      X=ABS(ALOG(D(I,J,2)/D(I,J,1)))
      IF (X.GT.0.34) K7=K7+1
      D(I,J,1)=D(I,J,2)
      S(I,J,1)=S(I,J,2)
      S(1,J,1)=S(1,J,2)
      D(1,J,1)=D(1,J,2)
  554 IF (W(I,J,3).GE.0.0) GO TO 558
      IF (I.LT.INT) GO TO 556
      S(I,J,2)=3.0*0.90*C11*W(1,J,3)**2/(C11*ABS(W(I,J,3))**3+1.0)**2
      IF (S(I,J,2).LT.0.001) S(I,J,2)=.001
```

```
      D(I,J,2)=C4*(C13*ABS(W(I,J,3))**3+1.0)
      IF (I.NE.INT) GO TO 560
      S(1,J,2)=3.0*0.45*C12*W(INT,J,3)**2/(C12*ABS(W(INT,J,3))
     1**3+1.0)**2
      IF (S(1,J,2).LT.0.001) S(1,J,2)=.001
      D(1,J,2)=C5*(C14*ABS(W(INT,J,3))**3+1.0)
      GO TO 560
  556 S(I,J,2)=3.0*0.45*C12*W(I,J,3)**2/(C12*ABS(W(I,J,3))**3+1.0)**2
      IF (S(I,J,2).LT.0.001) S(I,J,2)=.001
      D(I,J,2)=C5*(C14*ABS(W(I,J,3))**3+1.0)
      GO TO 560
  558 S(I,J,2)=0.0
      D(I,J,2)=C4
      IF (I.LT.INT) D(I,J,2)=C5
      IF (I.EQ.INT) D(I,J,2)=C5
  560 CONTINUE
      S( M3,ITN6,3) = ERROR
  562 IF (ITN6.GE.K2) GO TO 566
  564 IF(ITER .GT. K1) GO TO 735
      IF(T3.LT.C6)  GO TO 150
      IF (ERROR.GT.2) GO TO 150
  566 TIME=TIME+DELT
      ITN4=ITN4+1
      ITN3=ITN3+1
      WRITE (6,35) (S(M3,J,3) ,J=1,ITN6)
  567 WRITE (6,40) ITER,ITN6,ITN4,K7,K8
      WRITE (6,41) DELT,TIME,ERROR
      DO 572 J=2,N1
      DO 572 I=2,M1
      IF(W(I,J,1).GE.0.0) GO TO 568
      IF (I.NE.2) GO TO 568
      G(J)=-1.0
      GO TO 570
  568 IF(W(I+1,J,1).GE.0.0) GO TO 571
      X=I-2
      G(J)=X*A-A*W(I,J,1)/(W(I+1,J,1)-W(I,J,1))
  570 I=M1
      IF(J.EQ.N1)G(N)=G(N1)+(G(N1)-G(N2))*(R(N)-R(N1))/(R(N1)-R(N2))
      IF (G(N).LE.0.0) G(N)=0.
      GO TO 572
  571 IF(I.EQ.M1) G(J)=0.0
  572 CONTINUE
      WRITE (6,35) (R(J), J=2,N ,K5)
      WRITE (6,42) (G(J), J=2,N,K5)
      DO 574 K=1,M1
      I=M3-K
  574 WRITE (6,30) (W(I,J,1),J=2,N,K3)
      IF ( ITN3.LT.10)GO TO 605
      X=S(M,N1,3)
      DO 576 K=1,M1
      I=M3-K
      DO 575 J=2,N1,K3
  575 S(I,J,3) = S(I,J,3)/X
  576 WRITE (6,44) ( S(I,J,3) ,J=2,N1,K3)
      WRITE (6,25) X
      ITN3=0
      DO 579 K=1,M1
      I= M3-K
```

```
      DO 577 J=2,N1,K3
      S(I,J,3)= RAD/ (C11*ABS(W(I,J,1))**3 +1.)
  577 IF(W(I,J,1) .GE.0.0) S(I,J,3) = RAD
  579 WRITE(6,44) (S(I,J,3)   ,J=2,N1,K3)
      DO 584 K=1,M1
      I=M3-K
      X=I-2
      DO 580 J=2,N,K3
  580 S(I,J,3)=W(I,J,1)+A*X*COS(THETA)+SIN(THETA)*(R(N)-R(J))
  584 WRITE (6,30) (S(I,J,3),J=2,N,K3)
      DO 590 K=1,M1
      I=M3-K
  590 WRITE (6,44)(D(I,J,1), J=2,N,K3)
      DO 595 K=1,M1
      I=M3-K
  595 WRITE (6,44) (S(I,J,1),J=2,N,K3)
  605 XY=DELT
      DO 620 I=2,M
      Y= W(1,N,1)
      X=I-2
      IF(W(I+1,N,1).GE.0.)GO TO 610
      W(I,N,1)=W(I,N1,3)+(W(I,N1,3)-W(I,N2,3))*(R(N)-R(N1))/(R(N1)-R(
     1N2))
      XX=G(N)-X*A*COS(THETA)
      IF (W(I,N,1) .LT.XX) W(I,N,1)=XX
  610 IF(W(I,N,1).GT.Y)W(I,N,1)=Y
      IF(W(I,N,1).GE.0.) W(I,N,I)=0.
      W(I,N,2)=W(I,N,1)
  620 W(I,N,3)=W(I,N,1)
      IF (K8.GT.0) DELT=XY*C1
      IF (K9.GT.1) DELT=XY
      IF (K7.GT.1) DELT=XY/C1
      ITN6=0
      IF (ITN4.GT.1) T4=1.0
      IF (ITN4.GT. 3) T4=1.5
      T3= 0.0
      GO TO 150
  735 STOP
      END
```

APPENDIX B

MISCELLANEOUS INFORMATION

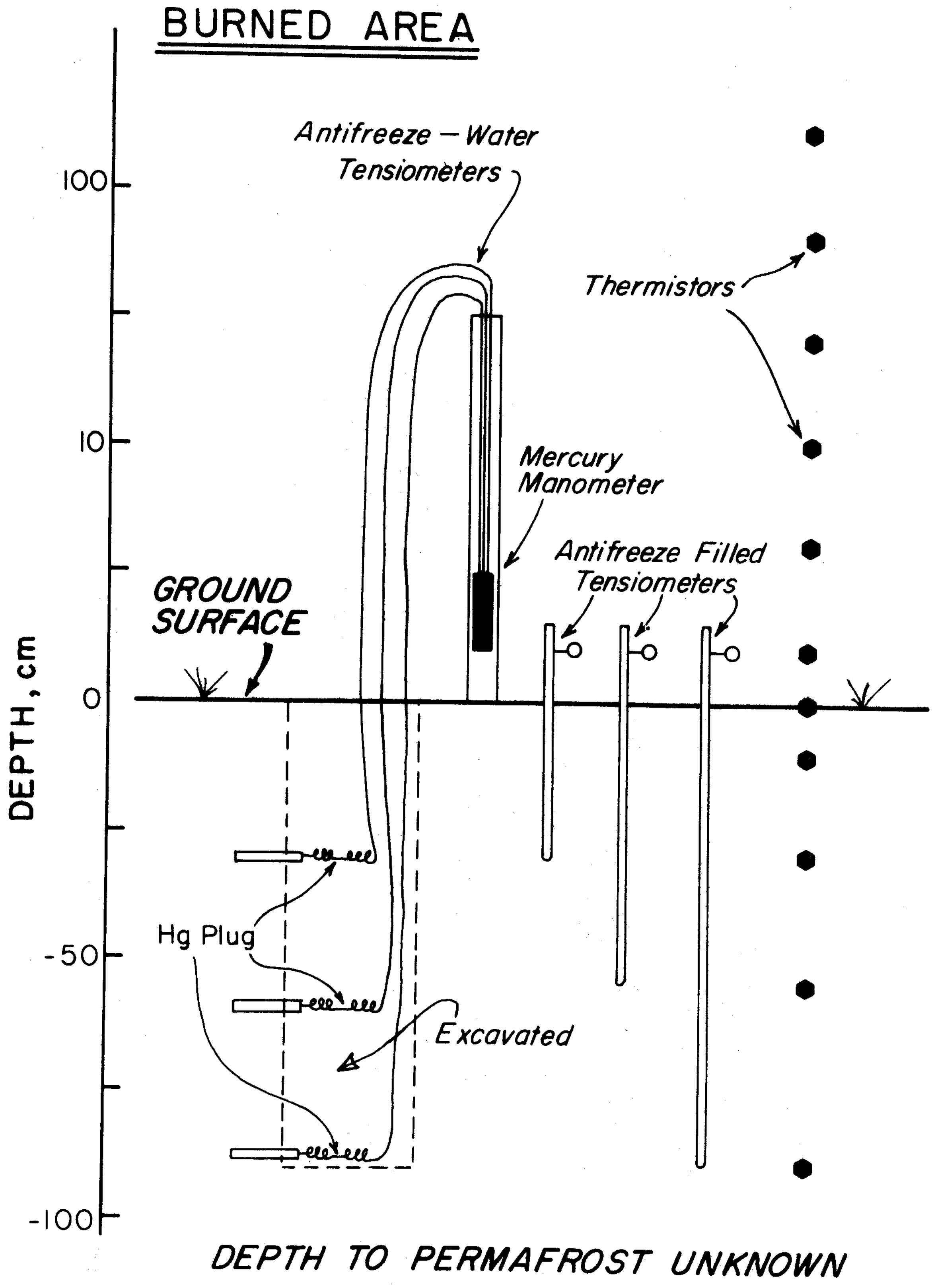

FIGURE B-1: The Layout of the Field Instrumentation at Site N-1.

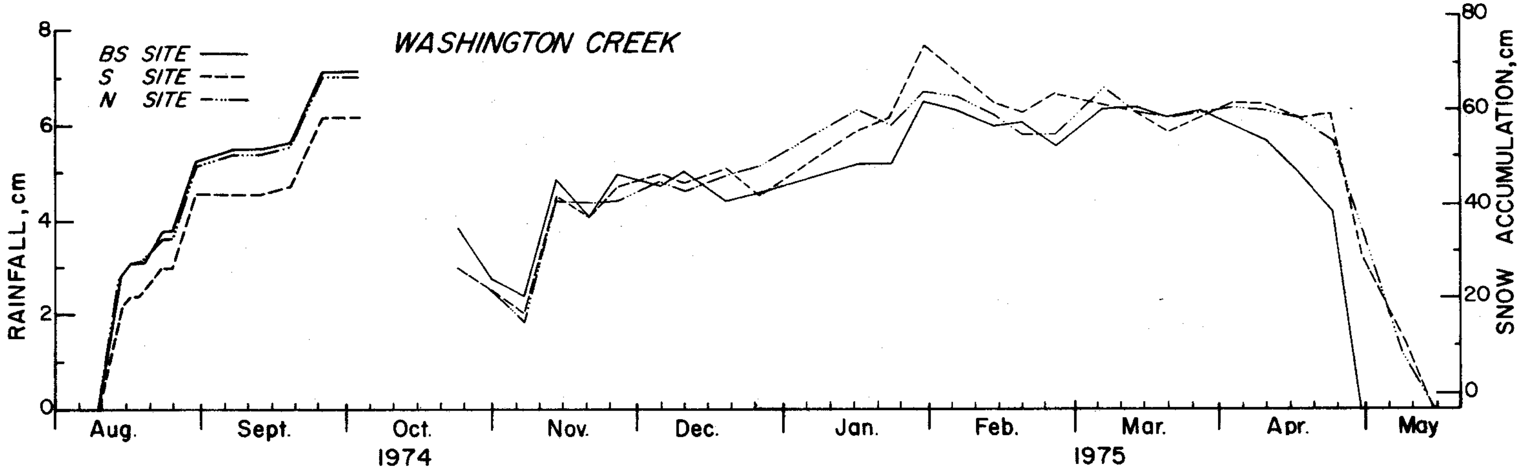

FIGURE B-2: The Accumulated Rainfall and Depth of Snowpack.

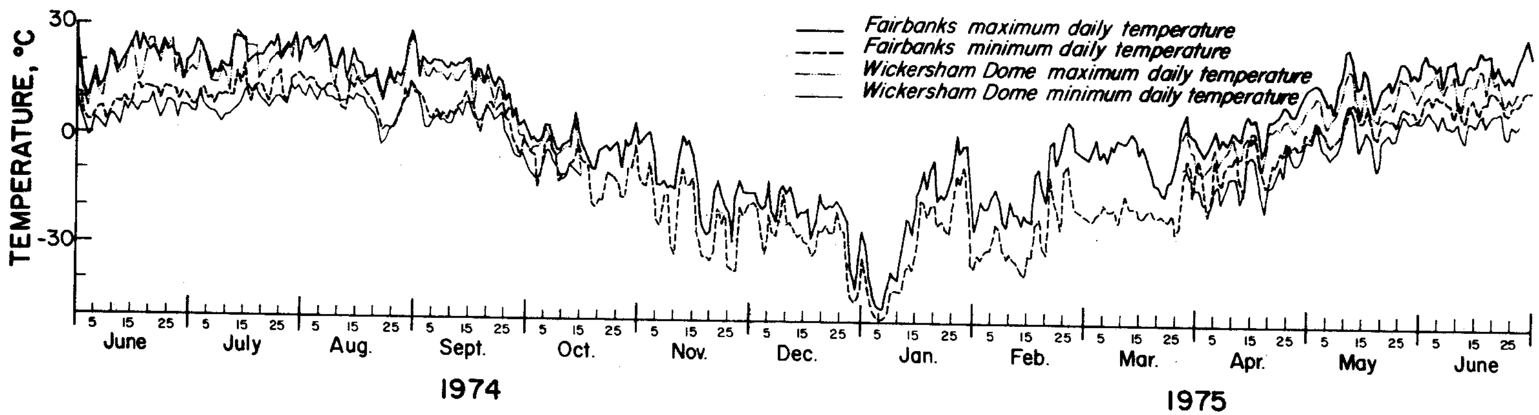

FIGURE B-3: Temperature Correlations at Wickersham Dome and at Fairbanks.

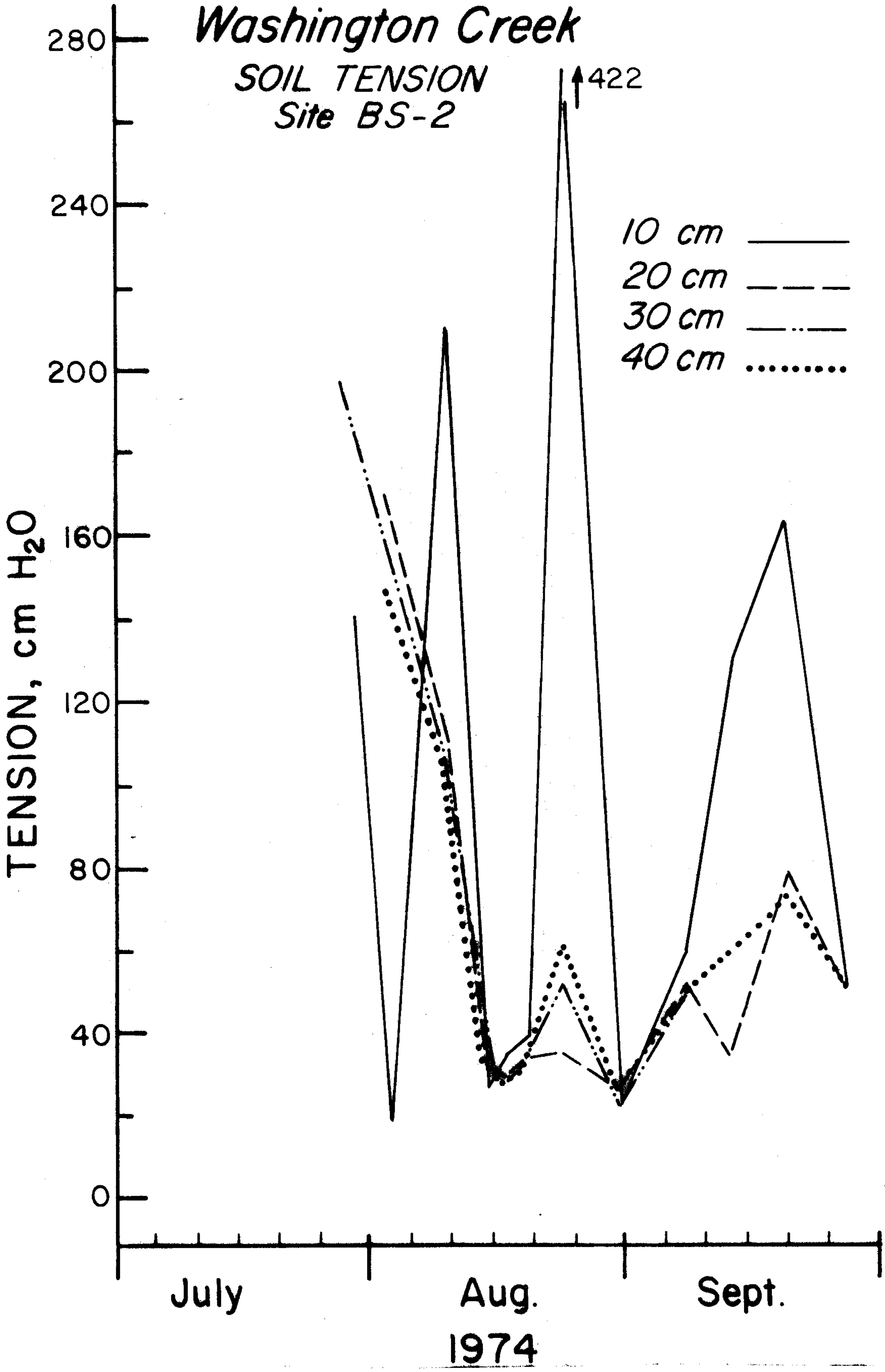

FIGURE B-4: Measured Soil Tensions at Site BS-2.

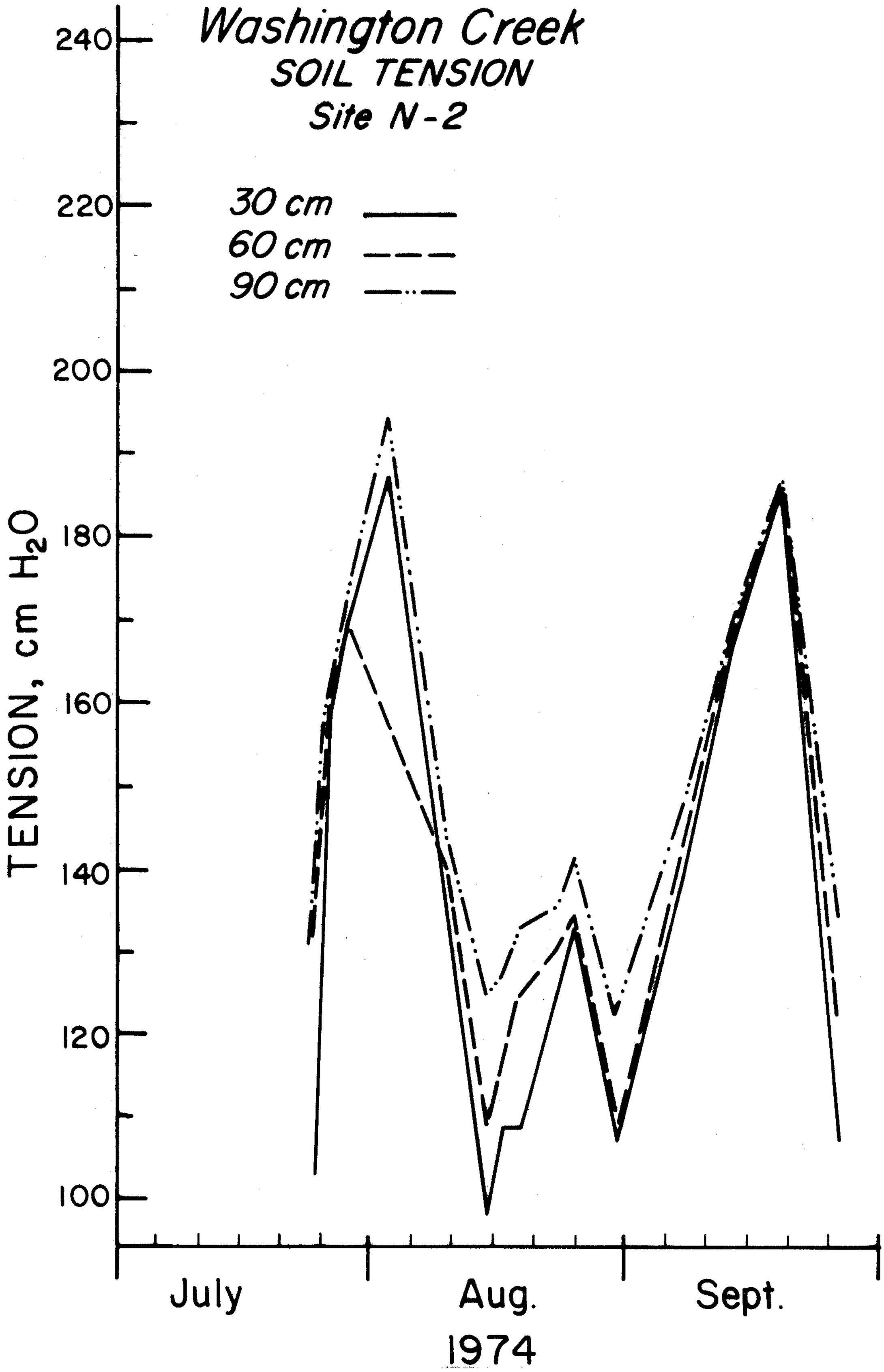

FIGURE B-5: Measured Soil Tensions at Site N-2.

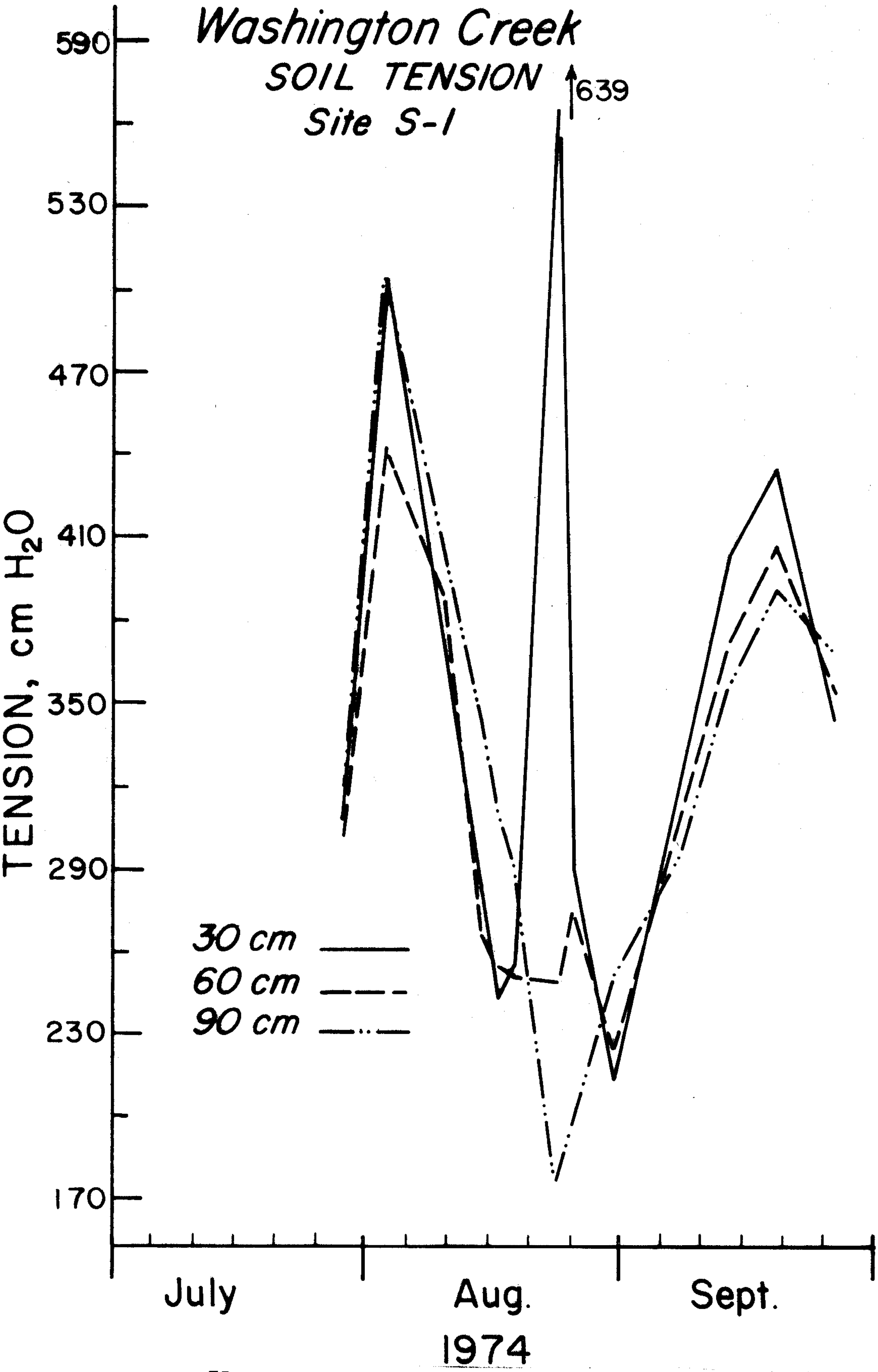

FIGURE B-6: Measured Soil Tensions at Site S-1.

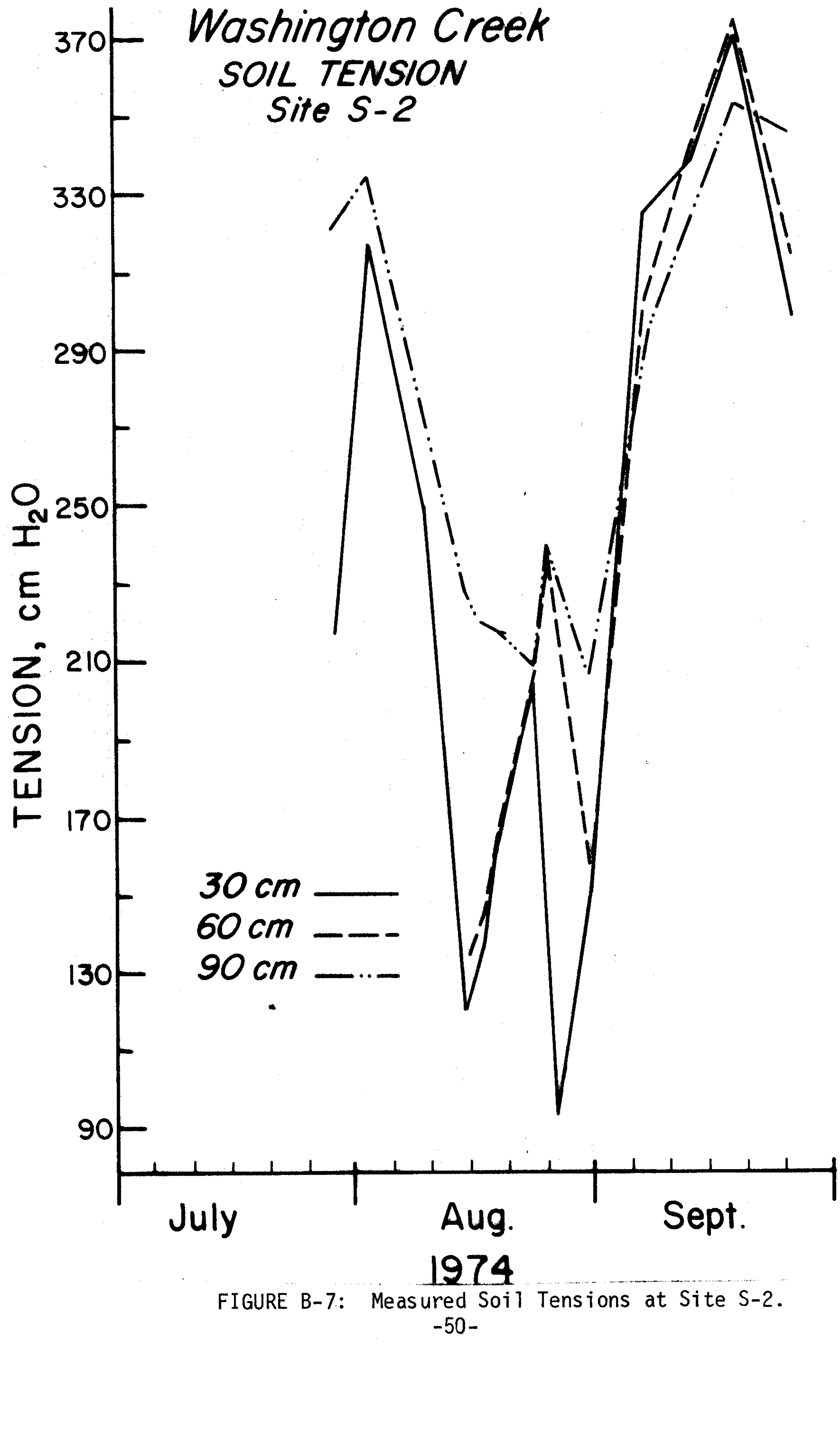

FIGURE B-7: Measured Soil Tensions at Site S-2.